Victoria Johansen

# Modification of glycosyltransferases in multiple myeloma

Master's thesis in Molecular Medicine
Supervisor: Siv Helen Moen
Co-supervisor: Tonje Marie Vikene Nedal

June 2021

**Master's thesis**

**NTNU**
Norwegian University of
Science and Technology

Victoria Johansen

# Modification of glycosyltransferases in multiple myeloma

Master's thesis in Molecular Medicine
Supervisor: Siv Helen Moen
Co-supervisor: Tonje Marie Vikene Nedal
June 2021

Norwegian University of Science and Technology
Faculty of Medicine and Health Sciences
Department of Clinical and Molecular Medicine

**NTNU**
Norwegian University of
Science and Technology

# Abstract

Multiple myeloma (MM) is a malignancy of the terminally differentiated B-cells, named plasma cells. The condition is characterized by clonal proliferation of plasma cells in the bone marrow. Almost all MM patients develop an osteolytic bone disease caused by a dysregulation in the bone remodeling process and up to 80% of patients have osteolytic bone lesions at the point of diagnosis. The bone disease is associated with severe bone pain and affects the patients' quality of life. Recent research indicates that the monoclonal immunoglobulins' (Igs), secreted by the myeloma cells, stimulates osteoclast differentiation/activation, and thereby promote bone loss. This effect is probably mediated by binding of Ig-aggregates to Fc receptors of osteoclasts; however, the mechanism is not fully understood. Aggregate formation is influenced by the Fc glycosylation of the Igs, and loss of terminal sialic acid and/or galactose in N-glycans might be responsible for their pro-osteoclastogenic effect. Addition of sialic acid and galactose residues take place in the Golgi apparatus and is mediated by glycosyltransferases (ST6Gal1 and B4GalT1). Reduced sialylation and galactosylation might be due to decreased expression of these glycosyltransferases. The overall aim of this project is to understand how altered glycosylation of Igs can affect the progression of MM bone disease and to improve current treatment of MM bone disease. The goal of this thesis was therefore to establish MM cell lines with modified expression of the glycosyltransferases ST6Gal1 and B4GalT1 for use in future *in vivo* studies. Additionally, the glycosylation of mouse serum Igs from a myeloma mouse model was analyzed. Gene and protein expression of ST6Gal1 and B4GalT1 was successfully modified in two MM cell lines, however, we were not able to conclude if these modifications resulted in altered sialylation/galactosylation of the Igs. The analysis of Ig glycosylation in the model showed a clear decrease in Ig sialylation compared to the healthy control. This mouse model might therefor be suitable to further investigate the effects of N-Acetylmannosamine (ManNAc) treatment.

# Sammendrag

Myelomatose, også kjent som beinmargskreft, er en kreftsykdom som kjennetegnes av ukontrollert vekst av plasmaceller i beinmargen. Nesten alle myelomatosepasienter utvikler en beinsykdom som følge av kreftsykdommen, og opptil 80% av pasientene har osteolytiske beinlesjoner ved diagnosetidspunktet. Beinsykdommen fører til store smerter i skjelettet og påvirker pasientenes livskvalitet. Den osteolytiske beinsykdommen er forårsaket av en dysregulering i oppbyggingen og nedbrytingen av bein. Nyere forskning indikerer at de monoklonale immunglobulinene (M-komponenten), utskilt av myelomcellene, stimulerer osteoklastdifferensiering/aktivering og på den måten fremmer bentap. Stimulering av osteoklaster skjer sannsynligvis ved binding av Ig-aggregater til Fcγ-reseptorer på osteoklaster, men mekanismen for hvordan denne signaleringen skjer er imidlertid ikke helt forstått. Kompleksdannelse er påvirket av Fc-glykosyleringen av immunglobulinene, og man tror at tap av terminal sialinsyre og/eller galaktose er viktig for deres osteoklastaktiverende effekt. Glykosylering av proteiner skjer i Golgi-apparatet og er katalysert av en gruppe enzymer som kalles glykosyltransferaser. Reduserer sialylering og galaktosylering kan skyldes redusert utrykk av de to glykosyltransferasene ST6Gal1 og B4GalT1. Det overordnede målet for dette prosjektet er å fremme forståelsen av hvordan endret glykosylering av immunglobuliner kan påvirke progresjonen av beinsykdommen forbundet med myelomatose og å forbedre dagens behandling av beinsykdommen. Målet med denne oppgaven var derfor å etablere myelomatosecellelinjer med modifisert utrykk av de to glykosyltransferasene ST6Gal1 og B4GalT1 til bruk i fremtidige *in vivo*-studier. I tillegg ble glykosyleringen av immunglobuliner fra en musemodell analysert. Vi lyktes med å modifisere gen- og proteinutrykket av ST6Gal1/B4GalT1 i to cellelinjer, men vi var ikke i stand til å konkludere om disse modifikasjonene resulterte i endret sialylering/galaktosylering av immunoglobulinene. Analysen av glykosyleringen av immunoglobuliner fra musemodellen viste en klar reduksjon i Ig sialylering sammenlignet med den friske kontrollen. Denne musemodellen kan derfor være en passende modell for å undersøke effekten av N-acetylmannosamin (ManNAc) behandling.

## Sammendrag

# Acknowledgement

# Table of contents

# Abbreviations

ACTB - Beta actin

ATP - Adenosine triphosphate

B4GalT1 - Beta-1,4-galactosyltrasferase

BMP - Bone Morphogenetic Protein

BMSC - Bone marrow stromal cells

BSA - Bovine Serum Albumin

CFBS - Carbo-Free Blocking Solution

c-Fms - Colony-stimulating factor

CTG - CellTiter-Glo

CTX-1 - Cross-linked C-terminal telopeptide of type I collagen

DAP12 - DNAX-activating protein of 12 kDa

DFDM - Non-fat dry milk

Dkk1 - Dickkopf1

DPBS - Dulbecco's Phosphate Buffered Saline

DTT - Dithiothreitol

ECA - Erythrina cristagalli

ER α-Man – Endoplasmic reticulum α-mannosidase

ERK - Extracellular-signal-regulated kinase

FBS - Fetal bovine serum

FCRγ - Fc receptor common γ subunit

FITC - Fluorescin isothiocyanate

FRET - Fluorescence Resonance Energy Transfer

FSC - Forward scatter

FucT - Fucosyltransferase

GalNac - N-acetylgalactosamine

GAPDH - Glyceraldehyde-3-Phosphate Dehydrogenase

GlcNAc - N-acetylglucosamine

GnT - N-acetylglucosamine transferase

HRP - Horseradish peroxidase

Ig - Immunoglobulin

IgAN - IgA nephropathy

IGH - Immunoglobulin heavy locus

IGHC – Immunoglobulin heavy chain constant domain

IL - Interleukin

ITAM - Immunoreceptor tyrosine-based activation motif

KD - Knockdown

LB - Luria-Bertani

LCA - Lens Culinaris Agglutinin

LDS - Lithium dodecyl sulfate

LTR - Long terminal repeat

M protein - Myeloma protein

ManNAc - N-Acetylmannosamine

MAPK - Mitogen-activated protein kinase

MB - Bone Marrow

M-CSF - Macrophage colony-stimulation factor

MGUS - Monoclonal gammopathy of undetermined clinical significance

MiRNA - MicroRNA

MM - Multiple myeloma

Neu5Ac - N-acetylneuraminic acid

Neu5Gc - N-glycolylneuraminic acid

NEAA - Non-Essential Amino Acids

NF-κB - Nuclear factor kappa B

NFATc1 - Nuclear Factor of Activated T Cells 1

OE - Overexpression

OPG - Osteoprotegrin

ORF - Open reading frame

OSCAR - Osteoclast-associated receptor

PAGE - Denatured polyacrylamide gel electrophoresis

PI - Propidium Iodine

PI3K - Phosphoinositide 3-kinases

ppGalNAc-Ts - Polypeptide GalNAc transferases

PS - Phospholipid phosphatidylserine

qPCR - Quantitative polymerase chain reaction

RA - Rheumatoid arthritis

RANKL - Nuclear factor κB ligand

RER - Rough endoplasmic reticulum

RISC - RNA-induced silencing complex

PLCγ = Phosphoinositide phospholipase Cγ.

RUNX2 - Runt-related transcription factor 2

SDS - sodium dodecyl sulphate

Ser - Serine

shRNA - Short hairpin RNA

siRNA - Small interfering RNA

SMM - Smoldering multiple myeloma

SNA - Sambucus nigra

SOC - Super Optimal Broth

SSC - Side scatter

ST3Gal - Beta-galactoside Alpha-2,3-sialyltransferse.

ST6GalNAc - Alpha-GalNAc Alpha 2,6-sialyltransferase

ST6GalT1 - Beta-galactoside Alpha-2,6-sialyltransferase 1

SV40 - Simian virus 40

Syk - Spleen tyrosine kinase

TAB = MAP3K7 binding protein

TAK - Transforming growth factor-β-activated kinase

Thr - Threonine

TNF-α - Tumornekrosefaktor-alfa

TRAF6 - TNF Receptor Associated Factor 6

VCAM-1 - Vascular cell adhesion molecule 1

VEGFR - Vascular endothelial growth factor

VSV-G - Vesicular stomatitis virus G protein

α-Glc - Alpha-Glucosidase

Note: For simplicity, the glycosyltransferases will be referred to as ST6GalT and B4GalT1 for both human and mice when referring to the proteins, and when referring to gene and protein expression collectively. When describing gene expression, standard rules for gene nomenclature in humans and mice are applied.

# 1. Introduction

## 1.1 Multiple myeloma

Multiple myeloma (MM) is a malignancy of the terminally differentiated B-cells, named plasma cells. The condition is characterized by clonal proliferation of plasma cells in the bone marrow (BM) (1). Under normal conditions, plasma cells play an important role in the humoral immune response by producing and secreting antigen specific antibodies. In MM, malignant plasma cells produce large amounts of monoclonal antibodies (M-proteins) (2). In more than 50% of patients the M-protein is immunoglobulins (Igs) of the IgG isotype. The second most common M-protein is IgA isotype, which makes up 20% of cases. The third major group of M-protein consists of light chain only ($\kappa$ and $\lambda$) and makes up 16% of cases (3). Clinical features of the disease are end-organ dysfunctions, including hypercalcemia, renal failure, anemia, and bone lesions, known as the CRAB features. In order to be diagnosed with MM, there must be > 10 % clonal plasma cells (PC) in the bone marrow (BM) or biopsy proven plasmacytoma in addition to one or more of the CRAB features (4). In 2019 there were 506 new cases of MM in Norway, of which 210 were female and 296 were male (5). The median age of diagnosis is about 70 years (6).

MM is thought to derive from an asymptomatic condition called monoclonal gammopathy of undetermined clinical significance (MGUS) that later evolves to smoldering multiple myeloma (SMM) which ultimately can lead to MM (6). In both conditions, none of the CRAB features are seen. In MGUS, clonal PCs make up < 10% of the BM and serum M-protein is < 30 g/l, while in SMM clonal PCs make up > 10% of the BM and serum M-protein is > 30 g/l (4). The risk for MGUS to develop into MM is estimated to be 1% per year and the risk for SMM to develop into MM is 10% per year for the first five years. After the first five years the risk is reduced (7), (8). MGUS is a relative common condition and is found in 3.2% of people older than 50 years (9). The initial genetic events that cause the formation of clonal plasma cells is either translocations affecting chromosome 14, specifically the immunoglobulin heavy (*IGH)* locus, or alterations in the number of chromosomes (hyperdiploidy) (10). Secondary genetic events are required for tumor progression and ultimately the progression of MGUS to MM, and include single-nucleotide variants, translocations and copy number variation in DNA-repair pathways and signaling pathways such as NF-$\kappa$B, MAPK and Myc (11), (12). There has been a rapid growth in available treatments options for MM patients the last

decades, and the five-year relative survival has increased. However, MM is still considered an incurable disease, as most patients relapse after one or more treatment regimens, as a result of drug resistance (13), (14), (15).

## 1.2 The bone disease of MM

Almost all MM patients develop an osteolytic bone disease, and up to 80% of patients have osteolytic bone lesions at the point of diagnoses. The bone disease is associated with severe bone pain and affects the patients' quality of life as well as their mortality. The osteolytic bone disease is caused by a dysregulation in the bone remodeling process, caused by increased osteoclast differentiation/activation and suppression of osteoblasts differentiation. This disruption ultimately leads to an increased resorption of bone and a decreased bone formation. The myeloma cells play a central role in the dysregulation of the bone remodeling process by altering the microenvironment of the BM. Myeloma cells secrete cytokines inhibiting osteoblast differentiation and pro-osteoclastic factors promoting osteoclast activation/differentiation (16), (17).

### 1.2.1   Bone remodeling

Bone remodeling is a continuous process of bone resorption and bone formation and is carried out by the different types of bone cells: osteoclasts, osteoblasts, and osteocytes (shown in Figure 1.1). Osteoclasts are large, multinuclear cells developed from hematopoietic progenitors and are responsible for bone resorption. By binding tightly to the bone, and secreting acid and enzymes (collagenase, protease, hydrolytic enzymes) the osteoclasts break down both the organic and inorganic matrix of the bone. Osteoblasts are monoclonal cells differentiated from mesenchymal stem cells and are responsible for bone formation. Osteoblasts secrete type I collagen and other proteins that serve as the organic matrix of the bone (osteoid). Following osteoid formation, osteoblasts secrete calcium and phosphate, which forms solid hydroxyapatite i.e., the inorganic matrix of the bone. Some osteoblasts become imbedded in the mineralized matrix, where they differentiate into osteocytes (18). Under normal conditions the osteocytes play a key role in the regulation of bone remodeling by sensing mechanical load and responding to stress by communicating with osteoblast and osteoclasts through dendritic processes in a neuron-like manner (19).
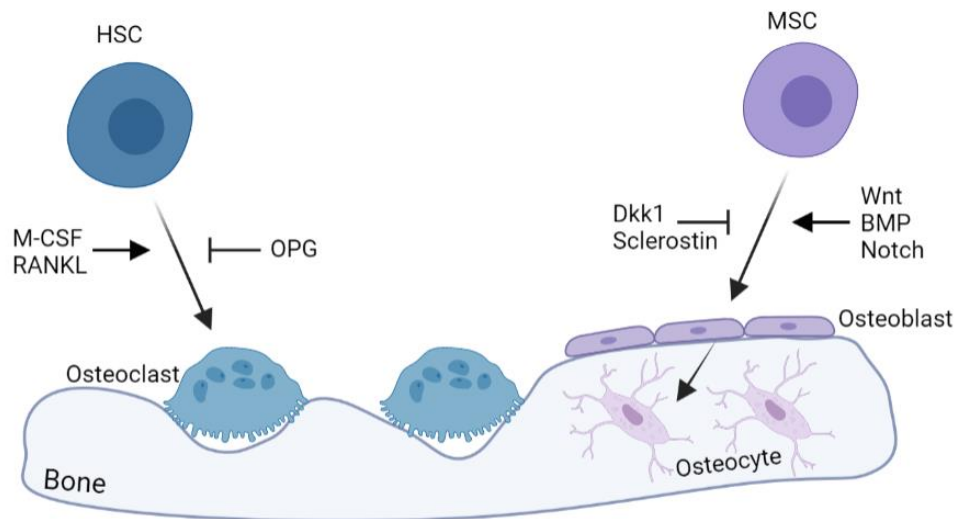
**Figure 1.1 Simplified figure showing the most important stimulatory and inhibitory factors/pathways in the differentiation of osteoclast and osteoblasts.** Macrophage colony-stimulation factor (M-CSF) and the receptor activator of nuclear factor κB ligand (RANKL) are two essential cytokines promoting osteoclastogenesis. Osteoprotegrin (OPG), a RANKL decoy receptor inhibits osteoclast differentiation. Osteoblast differentiation is dependent on the activation of Runt-related transcription factor 2 (RUNX2), which is regulated through the signaling pathways Wnt, BMP and Notch. Dickkopf1 (Dkk1) and sclerostin are inhibitors of Wnt signaling - and thereby inhibitors of osteoblast differentiation. Figure created with BioRender.com.

Bone remodeling is tightly regulated both locally and systematic. Systematic regulation primarily involves hormones (parathyroid hormone, calcitriol, growth hormone, thyroid hormones) and cytokines. Locally, a large number of growth factors and cytokines affecting osteoclast and osteoblast activation have been described (20). Differentiation of osteoblast is dependent on the activation of the transcription factor RUNX2. The three signaling pathways Wnt, BMP and Notch are all important regulators of RUNX2 activity (21), (22), (23). Osteoclast survival and differentiation is controlled by two essential cytokines: macrophage colony-stimulation factor (M-CSF) and the receptor activator of nuclear factor κB ligand (RANKL). M-CSF is expressed by osteocytes, osteoblasts, and bone marrow stromal cells (BMSC) and binds to colony-stimulating factor (c-Fms) receptors of osteoclasts, causing the activation of the ERK and Akt pathways, promoting cell proliferation and survival. RANKL is expressed/secreted by osteoblasts and activated T-cells and bind to the RANK receptor of osteoclast precursors. Binding of RANKL activates TNF receptor–associated factor 6 (TRAF6), which further activate several signaling pathways promoting differentiation of pre-osteoclasts into osteoclasts (24). Osteoprotegrin (OPG), secreted by BMSC and osteoblast act as a decoy receptor for RANKL and thereby inhibits osteoclastogenesis. In addition to the

cytokines M-CSF and RANKL, osteoclast differentiation is dependent on co-stimulatory signals from the activation of immunoreceptor tyrosine-based activation motif (ITAM) adaptor proteins Fc receptor common γ subunit (FcRγ) and DNAX-activating protein (DAP12) (25), (24) (Figure 1.2).
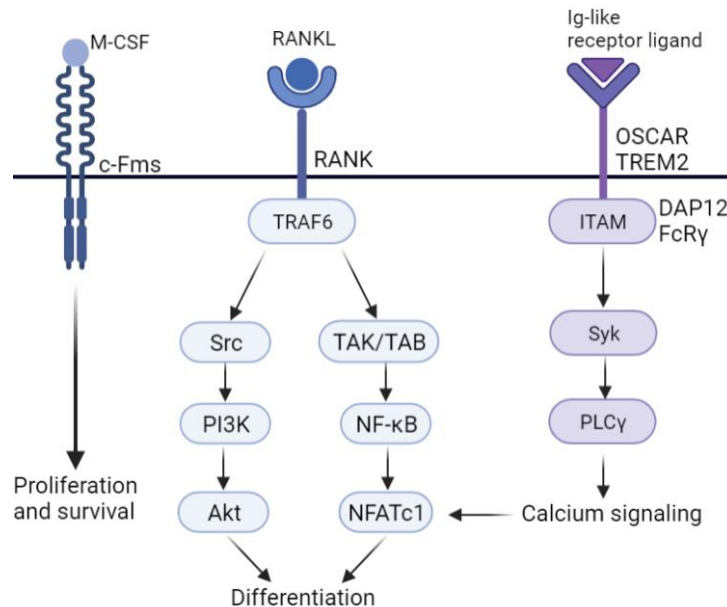


**Figure 1.2. Simplified figure showing essential signaling pathways required for osteoclast differentiation.** Binding of M-CSF to the c-Fms receptors, cause the activation of the ERK and Akt pathways, promoting cell proliferation and survival in pre-osteoclasts. Binding of RANKL to RANK activates TRAF6, which further activate several signaling pathways promoting the differentiation of pre-osteoclasts into osteoclasts. Activation of ITAM adaptor proteins FcRγ and DAP12 provide the co-stimulatory signal required for stable induction of NFATc1, mediated by calcium signaling. Figure adapted from (24) and created with BioRender.com

### 1.2.2 Disruptions in bone remodeling in MM

MM patients have an increased expression of RANKL and a decreased expression of OPG (26). The high RANKL/OPG ratio promote osteoclast differentiation. Myeloma cells also produce the chemokine MIP-1α, a potent inducer of osteoclast differentiation. MIP-1α increase the myeloma cell's ability to bind to BMSC, resulting in increased production of RANKL, VEGF, TNF-α and IL-6 in BMSCs. In addition to promoting osteoclast activation, myeloma cells also can block the differentiation of osteoprogenitor cells by blocking RUNX2 activity. MM patients with bone disease have an increased expression of Dickkopf1 (Dkk1) and sclerostin, which are inhibitors of the Wnt pathway (27), (16). Activation of the Wnt pathway is crucial for osteoblast differentiation.

### 1.2.3   Treatment options for MM bone disease

Treatments available today aim to reduce the survival/differentiation of osteoclasts and thereby reduce bone resorption. Bisphosphates are the standard treatment for MM bone disease today. Bisphosphates binds to mineralized bone and are taken up by osteoclasts during bone resorption, resulting in inhibited osteoclast activity. Treatment with bisphosphonates is associated with adverse events such as renal dysfunction, atypical femur fractures, osteonecrosis of the jaw (28). Denosumab, a monoclonal antibody targeting RANKL has shown promising results in clinical trials with MM patients. The drug is approved in the treatment of patients with osteoporosis and metabolic bone disease (29). Drugs targeting the inhibitors of osteoblast differentiation, DKK-1 and Sclerostin antagonists, are also currently being tested in clinical trials (28). As the bone disease of MM have a huge impact on both the patients' quality of life and mortality, there is a clear need for the development of new and more efficient drugs in the treatment of MM bone disease.

### 1.3 Glycosylation

Glycosylation of proteins is a post-transcriptional modification primarily taking place in the rough endoplasmic reticulum (ER), Golgi apparatus and cytoplasm. Glycosylation is important for protein stability and correct protein folding. The glycosylation status of a protein is also important when it comes to cell-to-cell interactions, specifically in immune cells. Two distinct types of protein glycosylation are N-linked and O-linked glycosylation. N-linked glycosylation is the attachment of a glycan to the nitrogen atom of an asparagine residue of a protein. N-glycans consists of a mannose and N-acetylglucosamine (GlcNAc) core, which might be fucosylated, and potentially have terminal galactose and sialic residues. O-linked glycosylation is the attachment of a glycan to the hydroxyl group of serine or threonine residues of proteins. O-glycans can consist of different monosaccharides in their core structure, where core one (mucin type) is the most abundant core structure, consisting of an initial N-acetylgalactosamine (GalNAc) residue. Numerous types of enzymes are involved in the process of glycosylation, and one important group of enzymes are glycosyltransferases. Glycosyltransferases catalyze the formation of a glycosidic linkage between two sugar molecules by transferring a monosaccharide from a nucleotide sugar (sugar donor) to an acceptor molecule (30), (31).

### 1.3.1 N-linked glycosylation

The biosynthesis of N-glycans takes place in the rough ER and Golgi apparatus (Figure 1.3) and begin with the assembling of a core structure consisting of two GlcNAc, nine mannose and three glucose residues attached to Dolichol-phosphate. The oligosaccharide is transferred onto the asparagine residue of the protein by the enzyme oligosaccharyltransferase (OST). The chain is then trimmed by α-glucosidase I and II (α-Glc I and II) and ER α-mannosidase (ER α-Man) in the lumen of the ER. The removal of the glucose residues allows the glycan to move from the ER to the Golgi apparatus. In the cis-Golgi the removal of mannose residues continues (mediated by α-mannosidases I and II). In medial-Golgi, GlcNAc transferases (GnT) catalyze the addition of GlcNAc residues to the oligosaccharide. In the trans-Golgi, core fucose and terminal galactose and sialic acid residues are added, catalyzed by fucosyltransferase, galactosyltransferase and sialyltransferase respectively (30). The end product showed in figure 1.3 is a complex type N-glycan, consisting of a fucosylated GlcNAc and mannose core and terminal galactose and sialic acid residues. This is the most abundant type of N-glycan in serum proteins (32). Other types of N-glycans are high-mannose N-glycans, which consist only of mannose residues, and hybrid N-glycans, which consist of a combination of antenna with terminal galactose and sialic acid residues and antenna with only mannose (30).
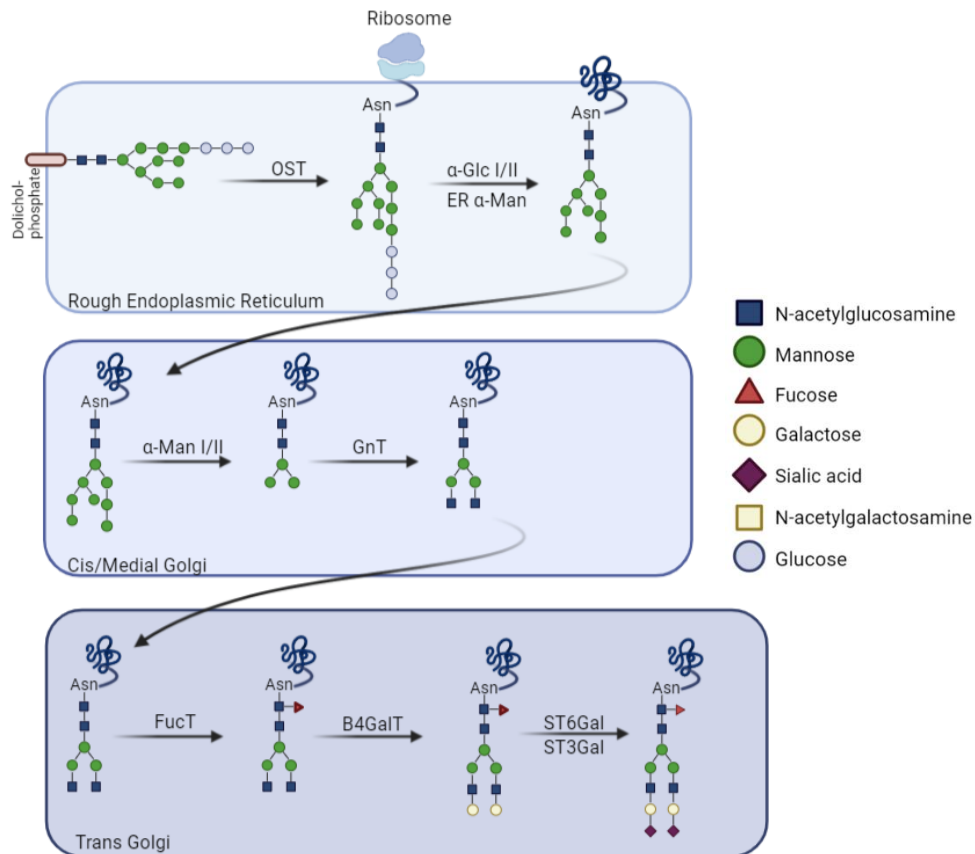
**Figure 1.3 Simplified figure of the biosynthesis of N-linked glycosylation of proteins taking place in the Rough Endoplasmic Reticulum and Golgi apparatus**. The removal of monosaccharides (braking of glycosidic bonds) is catalyzed by a group of enzymes called glycosidases. Glycosyltransferases transfer a monosaccharide from a nucleotide sugar (sugar donor) to an acceptor molecule. OST = oligosaccharyltransferase, α-Glc = Alpha-glucosidase, ER α-Man= ER Alpha-mannosidase, GnT = N-acetylglucosamine transferase, FucT = fucosyltransferase, B4GalT = Beta-1,4-galactosyltrasferase, ST6Gal = Beta-galactoside Alpha-2,6-sialyltransferase. ST3Gal = Beta-galactoside Alpha-2,3-sialyltransferase. Figure adapted from (30) and created with BioRender.com.

### 1.3.2   O-linked glycosylation

O-linked glycosylation can take place in the cytoplasm, rough ER, and the Golgi apparatus. However, the most common O-linked glycosylation observed in humans is the attachment of N-acetylgalactosamine (GalNAc) to Ser or Thr residues and this process takes place in the Golgi apparatus (Figure 1.4). These are called mucin type O-glycans and include most extracellular and secreted glycoproteins (including IgA1). The synthesis of mucin-type O-glycans is initiated by polypeptide GalNAc transferases (ppGalNAc-Ts), adding GalNAc to amino acid motifs. Additional monosaccharides are added as the protein moves through the Golgi apparatus (30). The galactosyltransferase core 1 B3GalT (C1B3GalT) catalyze the

linkage between galactose and GalNAc in a β1-3 linkage. Sialic acid can form glycosidic linkages with galactose, through a α2-3 linkage, and with GalNAc through a α2-6 linkage, catalyzed by the sialyltransferases ST3Gal1 and ST6GalNAc respectively (33).
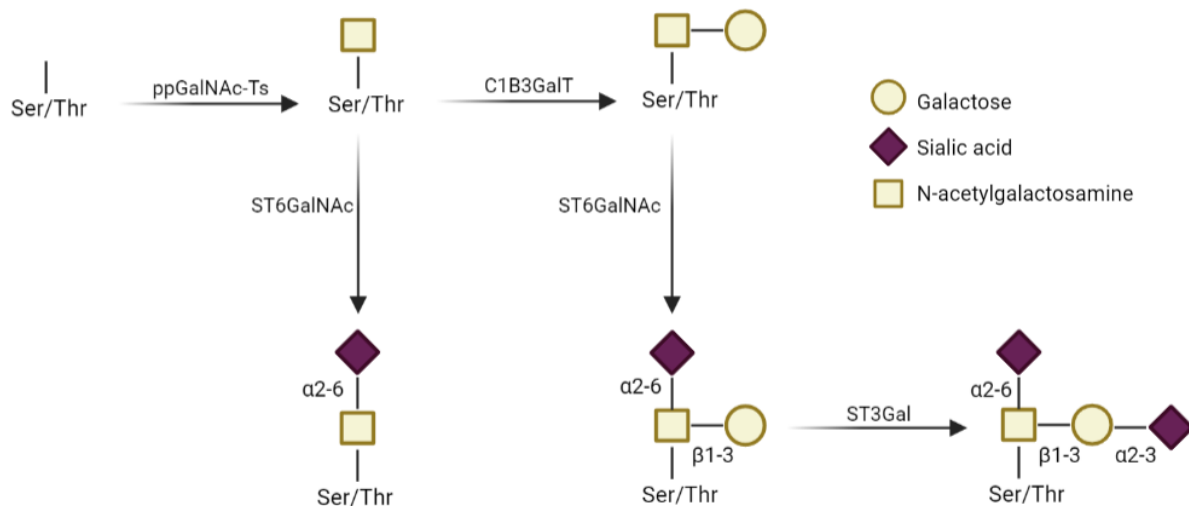


**Figure 1.4. Enzymes involved in the biosynthesis of type 1 O-linked glycans taking place in the Golgi apparatus.** The synthesis of type 1 O-glycans begin with the attachment of the N-acetylgalactosamine (GalNAc) core to serine or threonine residues of proteins. Galactose is added to the structure, followed by the attachment of sialic acid to GalNAc and/or galactose. If sialic acid is attached to GalNAc prior to galactose, this will block galactose from binding to the structure. ppGalNAc-Ts = Polypeptide GalNAc transferases, ST6GalNAc = alpha-GalNAc alpha 2,6-sialyltransferase, ST3Gal = Beta-galactoside Alpha-2,3-sialyltransferse. Figure adapted from (34) and created with BioRender.com.

## 1.4 Myeloma protein and immunoglobulin glycosylation

Myeloma protein (M protein) or the M component is the name of the monoclonal immunoglobulins produced by the myeloma cells. It is also commonly called the M spike and refers to the clear spike that appears in the gamma globulin zone when performing serum or urine electrophoreses. Immunoglobulins are glycoproteins and have seats for both N-linked and O-linked glycosylation. As mentioned, most MM patients secrete M proteins of IgG or IgA isotype. Figure 1.5 shows how IgA1 and IgG (subtype 1, 2, and 4) are glycosylated.

*IgG glycosylation*

The glycosylation status of IgG is widely studied. All IgG subtypes have N-glycosylation at a conserved asparagine at position 297 in the heavy chain constant domain 2 (CH2) (35). In addition, do IgG3 also have O-linked glycosylation. IgG N-glycans are biantennary glycans

consisting of a mannose and N-acetylglucosamine (GlcNAc) core, which might be fucosylated, and have terminal galactose and sialic acid residues.

*IgA glycosylation*

Human IgA show different glycosylation patterns in the two subtypes of IgA (IgA1 and IgA2). IgA1 heavy chain holds two seats for N-glycans per heavy chain, one in the CH2 domain and one in the tailpiece. The hinge region of IgA1 holds nine potential seats from O-glycans. Most seen are 4-5 O-glycans in the hinge region. The core structure of these O-glycans consists of a N-acetylgalactosamine (GalNAc) attached to a galactose in a β1-3 linkage. Sialic acid is commonly added to the O-glycan via a α2-3 linkage to galactose or via a α2-6 linkage to GalNAc. IgA2 do not have O-linked glycosylation but holds four conserved sites for N-glycans per heavy chain (36), (30), (33).
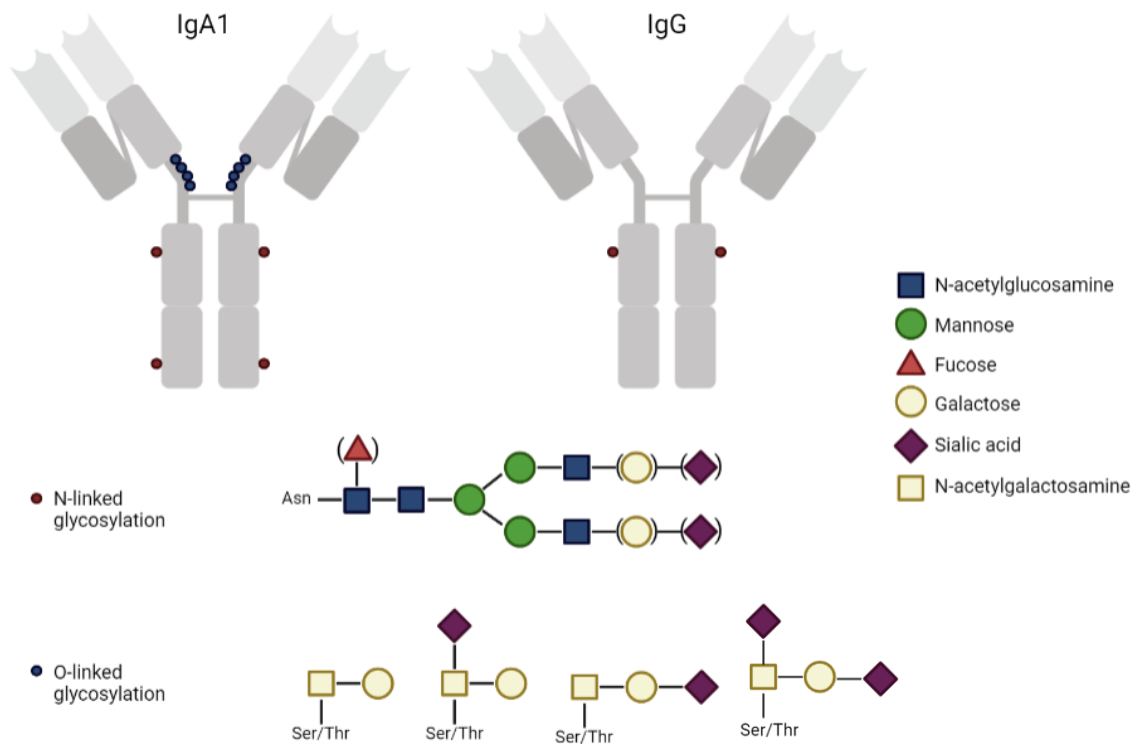


**Figure 1.5. Potential seats for O-linked and N-linked glycosylation in IgA1 and IgG (subtype 1,2 and 4) in humans.** IgG is N-glycosylated at a conserved asparagine at position 297 in the heavy chain constant domain (CH2). The hinge region of IgA1 holds nine potential seats from O-glycans. The core structure of these O-glycans consists of a type 1 core, N-acetylgalactosamine, attached to a galactose in a β1-3 linkage. Sialic acid is commonly added to the O-glycan via a α2-3 linkage to galactose or via an α2-6 linkage to N-acetylgalactosamine. Figure created with BioRender.com.

Mouse models are often used in studies examining the effects of glycosylation. Murine IgG have the same conserved seat for N-linked glycosylation as humans. O-linked glycosylation is observed in the hinge region of IgG2b isotype (37). The different subclasses of IgG (IgG1, IgG2a/b, IgG3) in mice show a greater diversity in sialylation and galactosylation than human IgG subclasses. N-linked glycosylation of the Fc region primarily consists of diantennary glycans with core fucosylation and a variable amount of galactose and sialic acid. The most prevalent form of sialic acid in mice is N-glycolylneuraminic acid (Neu5Gc), while humans predominantly express N-acetylneuraminic acid (Neu5Ac). In addition to subclass variations, it is also observed a greater variation in sialylation and galactosylation between different mice species compared to variation amongst humans (38), (39). Glycosylation of murine IgA is not widely studied but do like IgG hold conserved seats for N-linked glycosylation. Large variations are observed in especially the hinge region allele in different species of mice (40).

## 1.5 Immunoglobulins promoting bone loss

MM plasma cells produce large amounts of monoclonal Igs (M-protein). Recent research indicate that these Igs might also play a central role in the progression of the bone disease in MM (41). Bone loss is also seen in the autoimmune disease rheumatoid arthritis (RA). It is established that the autoimmune immunoglobulin (anti-citrullinated protein antibodies) complexes from RA patients stimulate bone loss in mouse models by promoting osteoclast differentiation (42), (43), (44). Osteoclast express Fcγ receptors and might therefore be affected by immune complexes. It was found that loss of terminal sialic acid residues in these autoantibodies might be responsible for their pro-osteoclastogenic potential, as only non-sialylated immune complexes stimulated osteoclastogenesis, both *in vivo* and *in vitro* (45). This is probably caused by the fact that the glycosylation status of the immunoglobulin, specifically IgG, influence their ability to bind to Fcγ receptors (46).

Most research regarding the effects of decreased sialylation and galactosylation is done on immunoglobulins of IgG isotype. It is well established that IgG Fc glycosylation affects the binding affinity to FcγR and IgG effector functions (47). Heavily sialylated and galactosylated IgGs has shown to have less affinity for FcγRs and thereby have an anti-inflammatory effect. Abnormal IgG Fc glycosylation is seen in both RA and systemic lupus erythematosus (SLE) and other autoimmune diseases (48), (49), (50). The impact of the glycosylation status of IgA

is not that well understood. Because IgA1 consists of both O-linked and N-linked glycosylation, there are more factors to take into consideration when studying IgA glycosylation. Decreased galactosylation of the O-linked glycans in IgA is seen in IgA nephropathy (IgAN) (51). These Igs are prone to self-aggregation (52). There is conflicting data of whether the glycosylation status of IgA affect its affinity for the FcαR (53), (54).

### 1.5.1    Abnormal glycosylation of immunoglobulins in MM

Previous research published by our research group has found that serum protein N-glycosylation differs between MM patients and healthy controls. Serum proteins from MM patients showed a decreased galactosylation and sialylation, and an increased fucosylation compared to healthy controls (measured by mass spectrometry) (32). In a newly published article, our research group found that immunoglobulins isolated from MM patients with bone disease promote osteoclast differentiation when added to human pre-osteoclasts *in vitro* (41). This effect was mediated by immune complexes or aggregates and not by monomeric immunoglobulins. As complex formation is influenced by the Fc glycosylation of the Igs, the glycosylation status of Igs from MM patients with and without bone disease was analyzed by mass spectrometry. The results revealed that the Igs from patients with bone disease were less galactosylated compared to MM patients without bone disease. When enzymatically adding galactose to bone disease derived Igs, they lost their pro-osteoclastogenic effect. Additionally, removing galactose from Igs derived from patients without bone disease made the Igs pro-osteoclastogenic. The study also demonstrated that Ig sialylation was reduced in 5TGM1 myeloma mice model upon disease progression. When treating the mice with N-acetylmannosamine (ManNac), a sialic acid precursor, the mice showed a reduced number of bone lesions and reduced tumor load compared to control mice treated with mannose. There was also found a reduction in serum Cross-linked C-terminal telopeptide of type I collagen (CTX-1) levels, indicating reduced osteoclast activity (41).

### 1.5.2    Regulation of protein glycosylation

How protein glycosylation is regulated is not fully understood, but the expression of glycosyltransferases in a cell can semi-quantitatively predict the cell surface glycan expression. This relationship might however be non-linear, and the mRNA expression of a glycosyltransferase might not correlate with the glycosylation of a protein. Post-transcriptional regulation of galactosyltransferases and other enzymes involved in

glycosylation probably play an important role in regulating protein glycosylation. MicroRNAs (MiRNAs) are thought to be a major post-transcriptional regulator of glycosyltransferases. Other factors such as turnover rates and enzyme activity also impact the glycosylation of proteins (55), (30). To explore the relationship between the expression of different glycosyltransferases and glycosylation status, our research group screened the expression of several glycosyltransferases involved in galactosylation and sialylation in plasma cells from MM patients with and without bone disease. We found significant lower expression of the two glycosyltransferases beta-galactoside alpha-2-6-sialyltransferase (ST6Gal1) and beta-1,4-galactosyltrasferase 1 (B4GalT1) in patients with bone disease compared to the patients without bone disease (41).

### 1.5.2.1 B4GalT1

Beta-1,4-galactosyltrasferase 1 (B4GalT1) is encoded by the gene *B4GALT1*, which is one of seven genes that encodes different glycosyltransferases in the B4GalT family. These enzymes encode type II membrane-bound proteins that catalyze the transfer of galactose from a nucleotide sugar (UDP-gal) to an acceptor sugar (GlcNAc, Glc, Xyln) in a beta1-4 linkage. The B4GalTs are differently expressed in different tissues. In regard to glycosylation of Igs, B4GalT1 is thought to be the main enzyme responsible for catalyzing the transfer of galactose to N-acetylglucosamine (GlcNAc) residues (56), (57), (58), (59).

### 1.5.2.2 ST6Gal1

Beta-galactoside Alpha-2-6-sialyltransferase (ST6Gal1) encoded by the gene *ST6GAL1* is a type II membrane protein that catalyze the transfer of sialic acid from CMP-sialic acid to a terminal N-glycan in an alpha 2-6 linkage (60). It is part of a superfamily of sialyltransferases made up of four families: ST3Gal, ST6Gal, ST6GalNAc and ST8Sia. There is only two known members of the ST6Gal family, ST6Gal1 and ST6Gal2. *ST6GAL1/St6gal1* is expressed in almost all tissues in both human and mice, while *ST6GAL2* expression is limited to particular tissues (61). Studies have also shown that ST6Gal2 utilize GalNacβ1-4GlcNAc as its preferred acceptor sugar (62), (63).

## 1.6 Lectins

Lectins are carbohydrate binding proteins that bind specifically to carbohydrates. In nature, lectins are found ubiquitously and they play an important role in cell-to-cell interactions.

Lectins usually have two binding sites for carbohydrates and therefore allow cross linkage between cells and macromolecules. Lectins with desired carbohydrate specificity have been purified from plants and other organisms to detect specific carbohydrates (64). *Sambucus nigra* (SNA) lectin is isolated from elderberry bark and binds specifically to sialic acid. The lectin is thought to bind to sialic acid attached to galactose or GalNAc in a α2-6 linkage, and to a lesser degree to sialic acid attached to galactose in a α2-3 linkage (65), (66). *Erythrina cristagalli* (ECA) lectin is purified from the seeds of the cockspur coral tree and binds primarily to galactose in a β1-4 linkage to GlcNAc (67). Lens Culinaris Agglutinin (LCA) lectin recognize the core of N-glycans by binding α-linked mannose residues and glucose. Binding might be enhanced by (α1-6) core fucosylation (65).

# 2. Aim

The overall aim of this project is to understand how altered glycosylation of Igs can affect the progression of MM bone disease to improve current treatment of MM bone disease. The goal of this thesis was therefore to establish MM cell lines with modified expression of the glycosyltransferases ST6Gal1 and B4GalT1 for use in future *in vivo* studies. Additionally, the glycosylation of serum Igs from a myeloma mouse model was analyzed by lectin blot, as this model was considered for *in vivo* studies examining the effect of ManNAc treatment.

The main objectives of the project were:

1. Knock down the expression of the glycosyltransferases ST6Gal1 and B4GalT1 in the cell line MOPC315.BM via lentiviral transduction utilizing shRNA.
2. Overexpress the glycosyltransferases ST6Gal1 and B4GalT1 in the cell lines JJN3 and MOPC315.BM via lentiviral transduction utilizing open reading frame (ORF) expression plasmids.
3. Characterize the expression of glycosyltransferases in modified cells at RNA and protein level and investigate if the modifications influence cell growth and survival in cell culture.
4. Analyze the glycosylation of proteins, especially immunoglobulins, in the modified cell lines by lectin blotting.
5. Analyze the glycosylation of serum immunoglobulins in a myeloma mouse model.

# 3. Materials and methods

## 3.1 Selecting appropriate cell lines for transduction

To understand of how altered glycosylation of immunoglobulins can affect osteoclast activation and promote bone loss, we wanted to alter the expression of the two glycosyltransferases ST6Gal1 and B4GalT1 in MM cell lines. The selection of suitable cell lines for modification, was performed before the start of this thesis. The research group examined the expression of the ST6Gal1, and B4GalT1 in several MM cell lines. Cell lines with relative high expression of ST6Gal1 and B4GalT1 were relevant for knockdown (KD), and cell lines with relative low expression of ST6Gal1 and B4Gal1 were relevant for overexpression (OE). How easily the different cell lines are transduced was also taken into consideration. The cell lines ANBL-6, INA-6 and MOPC315.BM were chosen for knockdown of *ST6GAL1/St6gal1* and *B4GALT1/B4galt1*. JJN3 and MOPC315.BM were chosen for overexpression of *ST6GAL1/St6gal1* and *B4GALT1/B4galt1*. The transduction of ANBL-6 and INA-6 was not successful and will not be described further in this thesis.

## 3.2 Cell culturing

In this thesis mainly two cell lines were used, MOPC315.BM, a MM mouse model, and JJN3, a human myeloma cell line. Both cell lines are known to cause osteolytic bone lesions. MOPC315.BM secrete IgA$\lambda_2$, commonly called M315 myeloma protein and JJN3 secrete (IgA)$\kappa$ light chain (68), (69), (70). Both cell lines were cultured in RPMI 1640 medium with L-glutamine (Sigma Aldrich, R8758) and 10% Fetal bovine serum (FBS) (Gibco 10270-106). In addition, the medium used to culture MOPC315.BM was supplemented with 1% MEM Non-Essential Amino Acids (NEAA) (Gibco, 11140050) and 1% sodium Pyruvate 100mM (Gibco, 11360070). The antibiotic Gentamycin (SANOFI, Gensumycin®, 40 mg/ml) was also added to this medium.

The cell lines were cultured in 37 °C in a humidified atmosphere consisting of 5% $CO_2$. The JJN3 cells were split twice a week and MOPC315.BM cells were split three times a week. The MOPC315.BM cells were usually split 1:10, 1:20 or 1:30, trying to never let them pass 0.5 mill cells/ml. JJN3 cells were usually split down to a concentration of 0.02 or 0.04 mill cells/ml. BECKMAN COULTER Z2 coulter counter® Particle Count and Size Analyzer was used for counting the cells.

### 3.2.1 Selection media

After lentiviral transduction, ST6Gal1 and B4GalT1 KD/OE, and controls were cultured in selection medium. MOPC315.BM ST6Gal1/B4Gal1 KD and OE were cultured in medium with 4 µg/ml puromycin (Sigma-Aldrich, 540222) for two weeks, before the dose was reduced to 2 µg/ml puromycin. JJN3 cells with ST6Gal1 OE were cultured in medium with 25 µg/ml of Blasticidin (Invivogen, ant-b1), and JJN3 cells with B4GalT1 OE were cultured in medium with 0.5 µg/ml Puromycin. The dose of blasticidin was later reduced to 5 µg/ml.

### 3.2.2 Cloning of MOPC315.BM

MOPC315.BM cells were transduced with transduction ready *B4galt1 and St6gal1* shRNA lentiviral particles. After one week the cells were cloned by limiting dilution. Concentrations of 0.5, 1, 2, and 4 cells per well were seeded out in 96 well plates. After incubation for 24 hours (37 °C, 5% $CO_2$) each plate was examined under the microscope, counting, and marking the wells with only one or two cells. These wells were observed further and as the cell population grew, the cells were moved to 24 well plates and later to 25 $cm^2$ flasks. The clones were given names to distinguish between control clones (MC), ST6Gal1 KD clones (MST) and B4GalT1 KD clones (MB).

### 3.2.3 Harvesting cells

When harvesting cells for western blots and lectin blots, a suitable number of cells (usually about 2.5 million cells) was collected and centrifuged (8 minutes, 1500 rpm, 4 °C). The supernatant was removed before the cells were washed in cold Dulbecco's Phosphate Buffered Saline (DPBS) (Sigma, D8537). The cells were then pelleted by centrifugation (5 minutes, 800 x *g*, 4 °C*).* For RNA isolation, the cells were pelleted without the DPBS wash and in pellets of about 0.5 million cells. The dry pellets were stored at -80 °C.

### 3.2.4 Harvesting supernatant for lectin and western blots

The cells were centrifuged for 8 minutes at 1500 rpm, washed in HANKS (Sigma, H9269), and resuspended in fresh media without FBS. The cells were cultured for 24 hours before harvesting the supernatant. In some experiments the cells were cultured in 0.5% BSA for 24 hours before harvesting the supernatant. When harvesting the supernatant, the cells were centrifuged for 5 minutes at 1500 rpm in 4 °C and the supernatant was moved to a new tube and frozen at -20 °C.

### 3.2.5   Calculation the doubling time

The doubling time of the transduced cells was calculated using the following formula. The MOPC315.BM cells were split to a concentration of 0.02 million cells per ml and grown for 48 hours before being counted. JJN3 cells were split to a concentration of 0.02/0.04 million cells per ml and grown for 72 hours before being counted.

$$DoublingTime = \frac{duration * \log(2)}{\log(FinalConcentration) - \log(InitalConcentration)}$$

### 3.3 Lentiviral transduction

Lentiviral transduction was utilized to overexpress and knock down the two glycosyltransferases ST6Gal1 and B4GalT1 in the cell lines MOPC315.BM and JJN3. Firstly, ST6Gal1 and B4GalT1 was knocked down in MOPC315.BM, utilizing transduction ready *B4galt1/St6gal1* short hairpin (sh) RNA Lentiviral particles purchased from Santa Cruz Biotechnology. This transduction was performed by other members of the research group and the method itself will not be described in this thesis, but the following paragraph will give a short summary of the principle of gene silencing utilizing shRNA. Later, ST6Gal1 and B4GalT1 were overexpressed in JJN3 and MOPC315.BM by utilizing open reading frame (ORF) expression plasmids. The plasmids were first propagated in E. coli, followed by a purification (described in 3.3.4), before being co-transfected with GeneCopoeia Lenti-Pac HIV Expression Packaging kit into HEK293T cells (described in 3.3.6). The virus containing cell supernatant was then harvested and used to transduce JJN3 and MOPC315.BM (section 3.3.8).

### 3.3.1   Gene knockdown by transduction of shRNA

shRNA is a type of RNA interference that can be utilized to silence the expression of specific genes. Introducing the shRNA into the target cell via a viral vector allows for stable integration of shRNA and a long-term gene knock down (Figure 3.1). The shRNA is continuously expressed in the cell and upon entering the cytoplasm, the loop is cleaved by the enzyme Dicer, transforming the shRNA into a small interfering RNA (siRNA). The siRNA consists of a guide stand and a passenger strand. The guide strand associates with RNA-induced silencing complex (RISC) while the passenger strand is degraded. As the guide strand pairs with the (target) complementary mRNA molecule, the mRNA molecule is cleaved and rapidly degraded in the cell, preventing the mRNA from being translated (71).
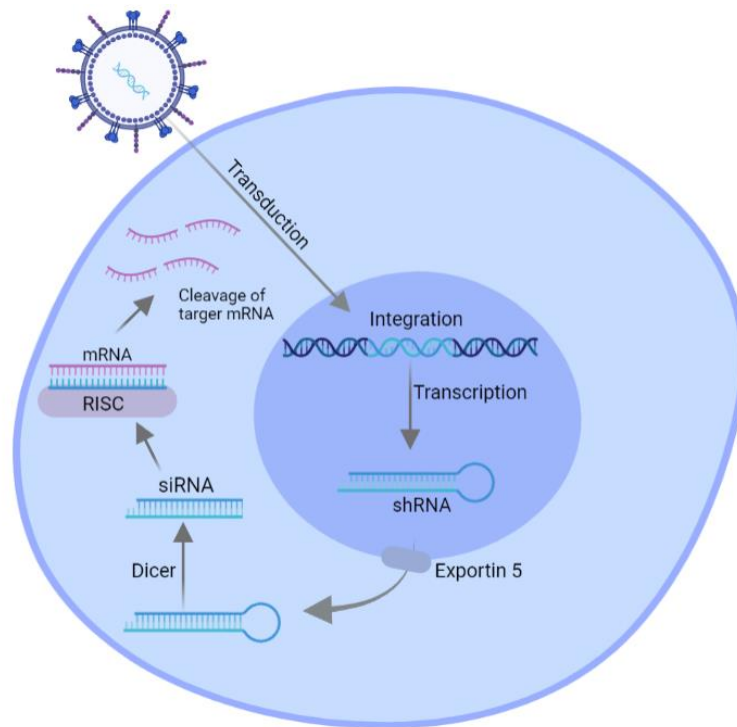
**Figure 3.1. Simplified figure of how shRNA silences the expression of a target gene**. shRNA is expressed and transported out of the nucleus via exportin 5. In the cytoplasm the shRNA is cleaved by the enzyme Dicer, transforming the shRNA into small interfering RNA (siRNA). The passenger strand is degraded while the guide strand is associated with RNA-induced silencing complex (RISC). As the guide strand pairs with the target mRNA, the mRNA is cleaved and degraded. Figure created with BioRender.com.

### 3.3.2 Principle of transformation (E. coli)

Transformation is a type of horizontal gene transfer, where the bacteria take up foreign DNA from the surroundings. Two different methods are used to transform bacteria in the lab, electroporation, and chemical transformation. In this thesis, chemical transformation was utilized. The E. coli cells used in this method are chemically competent cells, meaning they are treated with a cation e.g., calcium, to increase the permeability of the bacterial cell wall and membrane. To increase the permeability further, the mixture of bacteria and plasmid undergo a heat shock, where the mixture is quickly heated and cooled down. This process causes the formation of pores in the membrane, allowing the plasmid to enter the cell. After the incorporation of the plasmid, the bacteria need a recovery period, where the pores in the membrane are repaired and the antibiotic resistant gene (from the plasmid) is expressed. SOC medium is a commonly used medium to maximize the transcription efficiency. Luria-Bertani (LB) medium is another rich medium that can be utilized, although this might in some cases reduce the efficacy of the transformation. After the recovery period in either SOC medium or

LB medium the cells are plated on LB agars containing an antibiotic (e.g., ampicillin). Only the transformed cells, containing a resistance gene against the specific antibiotic will grow on the agar plate (72), (73), (74).

### 3.3.3 Principle of plasmid purification

To utilize the plasmids propagated in E. coli, they need to be purified, meaning all the other components of the bacterial cell needs to be removed. In this thesis, PureYield Plasmid Miniprep System by Promega was used. This first step of this procedure is the lysis of the bacterial cells. The lysis buffer consists of the detergent sodium dodecyl sulphate (SDS) and sodium hydroxide, which raises the pH of the sample. The detergent lyses the cell membrane, releasing the cell components. The high pH causes the denaturation of the proteins and chromosomal and plasmid DNA. After a short mix, the neutralization buffer is added. Because of their small size, the plasmid DNA can efficiently base pair again. The chromosomal DNA, proteins, and cellular debris, however, will aggregate and form a white precipitate. The aggregate is removed by centrifugation. The plasmid is further purified by using a silica membrane column. Plasmid DNA will bind to the silica membrane, whereas the contaminants are flushed trough via centrifugation. Promega's procedure also includes an Endotoxin Removal Wash, which removes RNA, protein, and endotoxin contaminants. When adding an elution buffer with low ionic strength, the RNA will release from the silica membrane (75), (76).

### 3.3.4 Transforming E. coli and Plasmid purification

Heat shock competent E. coli cells (DH5α) were used to propagate the plasmids purchased from GeneCopoeia. 0.25-0.68 ng of plasmid was added to 50 µl of E. coli followed by an incubation on ice for 10 minutes. After the incubation, the cells were moved to a heating block holding 42 °C, for 45 seconds. Thereafter, the cells were cooled on ice for two minutes before adding 180 µl of LB medium followed by an incubation for one hour at 37 °C. The cells were seeded out on LB agar plates, containing 50 µg/ml of ampicillin, in the dilutions 1:1 and 1:100. The plates were incubated over night at 37 °C. The next day, a single colony (from each plasmid) was transferred to LB medium. The bacterial suspensions were incubated in a shaking incubator overnight (37 °C, 250 rpm). The next day, the plasmids were purified utilizing PureYield Plasmid Miniprep System (Promega, A1222), following the manufacturer's procedure called "DNA purification by centrifugation". DNA concentration of

the purified plasmids was measured using NanoDrop ND-1000 spectrophotometer (Thermo Fisher).

### 3.3.5   Principle of transfection (HEK293T)

Transfection is the method used to introduce nucleic acids into a cell via non-viral methods. In this thesis, a lipid-based transfection method was utilized to introduce the viral genes needed to produce lentiviral particles. The GeneCopoeia Lenti-Pac HIV Packaging system used in this thesis is a third generation, self-inactivating lentiviral vector system. The gene of interest is packed into lentiviral vectors by co-transfecting the ORF expression plasmid and GeneCopoeia Lenti-Pac HIV Expression Packaging plasmids into HEK293T cells. HEK293T cells are immortalized human embryonic kidney cells that express simian virus 40 (SV40) large T antigen. Transfected plasmids with an SV40 origin of replication can be replicated in these cells.

In a third-generation lentiviral packaging systems, the viral genome is split into four plasmids (77). The ORF expression plasmid consists of all the elements required for a stable integration of the lentiviral expression constructs into genomic DNA. The U3 region of the 5' long terminal repeat (LTR) is replaced by an RSV promotor. This results in a Tat-independent transcription of viral RNA. At the U3 region in the 3' LTR there is a deletion in the enhancer, causing the self-inactivation of the lentiviral construct after reverse transcription and integration. The ORF expression plasmid lacks the elements required for transcription and packing of an RNA copy of the ORF into viral particles. These elements are provided by the packaging mix. The Lenti-Pac HIV packaging mix is a mixture of plasmids containing the regulatory gene *rev*, and the genes required for packaging, *gag,* and *pol.* The genes are expressed from different plasmids lacking packaging signals. Therefore, none of these genes will be present in the packed lentiviral genome, making the lentiviral particles replication incompetent. The packaging mixture also include an envelope plasmid. To broaden the tropism of the lentivirus, the envelope protein HIV-1 env glycoprotein is replaced with vesicular stomatitis virus G protein (VSV-G) (78), (79).

### 3.3.6   Transfection of HEK293T cells

The day before the transfection, 650 000 HEK293T cells were seeded out in 3 ml of DMEM (BioWhittaker, 12-604F) with 10% FBS. The cells were incubated overnight in 37 °C with 8% $CO_2$. The next day the medium was changed, and the cells were moved into the virus lab.

The DNA/EndoFectin Lenti complex was made by preparing two solutions in separate tubes. The first solution was made by adding 0.92 µg of lentiviral ORF expression plasmid and 1.85 µl of Lenti-Pac HIV mix to 74 µl Opti-MEM® (Invitrogen, 31985-062) in a sterile polypropylene tube. The second solution was made by diluting 5.6 µl of EndoFectin Lenti into 74 µl of Opti-MEM®. Thereafter, the EndoFectin Lenti solution was added dropwise to the DNA solution, while gently mixing the tube. The mixture was incubated for 10 minutes at room temperature before being added to the dish holding the HEK293T cells. The cells were incubated overnight (37 °C, 5% $CO_2$). The following day, the media was replaced with fresh DMEM containing 10% FBS and 1x TiterBoost. The lentiviruses were harvested the next day by centrifuging the media at 500 x $g$ for 10 minutes followed by a filtration of the supernatant trough a 0.45 µl polyethersulfone (PES) low protein-binding filter.

### 3.3.7 Principle of transduction

Transduction is the method used to introduce DNA into a cell via a viral vector. Enveloped viruses have viral fusion proteins on their surface, allowing them to fuse with the membrane of the host cell and release the viral genome into the cell. In this case, the lentiviral particles produced by HEK293T cells contain an expression construct with the genes and promotors required for a stabile expression of the ORF. In addition, the expression construct contains the genes providing the antimicrobial resistance. A successful transfection will lead to a stabile integration of these genes into the genome of the target cells. Polybrene is added to the media to increase the infection efficacy by neutralizing the repulsing charges between the viral particle and the cells. After the transduction, cells are grown in appropriate selection media to ensure the survival of only the transduced cells (80).

### 3.3.8 Transduction of MOPC315.BM and JJN3 (ORF expression plasmid)

MOPC315.BM and JJN3 were seeded out in 250 µl of medium in a 12-well plate with 200 000 cells per well (the media used is described in 3.2 Cell culturing). 50 µl of Polybrene (Sigma-Aldrich, H9268) was added to each well. The virus supernatant was added to the target cells in two dilutions, 1:2 and 1:10. For the mock well controls, 50 µl of Polybrene was added instead of the virus supernatant. The cells were incubated overnight at 37 °C in 5% $CO_2$. The next day, the supernatant was removed, and the cells were given new medium with either puromycin or blasticidin (see table 3.1) and without Polybrene. The optimal concentration of puromycin and blasticidin in the selection media was analyzed by other

members of the research group prior to transduction. After one week the eGFP controls were analyzed via flow cytometry, determining the amount of eGFP positive cells.

Table 3.1. A list of the plasmids used in the lentiviral transduction of MOPC315.BM. and JJN3 and their appropriate selection medium.

| Plasmid | Cell line transduced | Selection media |
|---|---|---|
| 0. eGFP-control plasmid | JJN3 and MOPC315.BM | No selection |
| 1. Ex-neg-LV105 Empty | JJN3 and MOPC315.BM | Puromycin |
| 2. Ex-neg Lv197 Empty | JJN3 | Blasticidin |
| 3. Ex-mo-351-LV197 ST6GAL1 | JJN3 | Blasticidin |
| 4. Ex-co-234-LV105 B4GALT1 | JJN3 | Puromycin |
| 5. Ex-mm05221-LV105 St6gal1 | MOPC315.BM | Puromycin |
| 6. Ex-mm02717-LV105 B4galt1 | MOPC315.BM | Puromycin |

## 3.4 Real-Time quantitative PCR

In this thesis, Real-Time quantitative PCR (RT qPCR) was used to analyze the gene expression of the genes *B4GALT1/B4galt1* and *ST6GAL1/St6gal1* in MOPC315.BM KD/OE cells and JJN3 OE cells. The first qPCR after the transduction gave an indication of whether the KD/OE of *B4GALT1/B4galt1* and *ST6GAL1/St6gal1* had been successful or not. After this initial qPCR, the KD/OE cells were tested frequently to assure there were no changes in the expression of the glycosyltransferases. In order to analyze the expression of the glycosyltransferases, RNA was isolated (3.4.2), followed by cDNA synthesis (3.4.4) and lastly qPCR (3.4.6).

### 3.4.1  Principle of RNA isolation

The goal of RNA isolation is to end up with pure RNA, meaning there is no proteins, DNA, lipids, or carbohydrates in the sample. In this thesis, a column-based method was utilized. RNA longer than 200 bases binds to the RNeasy silica membrane in the spin column under the appropriate conditions. Before the process of RNA isolation can occur, the RNA is made accessible by lysing the cells. The RLT lysis buffer (Qiagen, 79216) used in this project, consists of guanidine isothiocyanate, which inactivates RNases, and thereby protects RNA from degradation. DNase, which cleave single and double stranded DNA is added to assure a DNA free product. Ethanol is added to the sample to provide the proper conditions for the RNA to bind to the silica membrane. Other cell components are washed away by centrifugation. The sample is washed one time with RW1 buffer, which helps to remove cell

components e.g., carbohydrates and proteins that are non-specifically bound to the membrane. Further, the sample is washed twice in RPE buffer, which removes traces of salt. Lastly, the sample is eluted in water (81).

### 3.4.2   RNA isolation procedure

RNA was isolated using the QIAcube (Qiagen), an instrument designed to automize the process of RNA/DNA isolation. RNeasy® Mini kit (Qiagen, 74104) was utilized, and run with the protocol named "Purification of total RNA from Animal tissues and cells including DNase digestion". Samples were placed on ice as soon as the procedure was done and kept on ice until storage in a -80 °C freezer. RNA concentration and quality were measured using NanoDrop ND-1000 spectrophotometer.

### 3.4.3   Principle of first strand cDNA synthesis

Complementary DNA (cDNA) is synthesized from an RNA template via reverse transcription. This process is catalyzed by a group of enzymes called reverse transcriptases. cDNA is more stable than RNA and allows for further analysis, such as qPCR. In this project, qPCR and cDNA synthesis were performed in two separate steps and the cDNA produced is first strand cDNA. To transform all mRNA into cDNA, a mix of random octamers and oligo(dT) primers are used to provide a starting point for the reverse transcriptase. cDNA synthesis consists of three steps: primer annealing, DNA polymerization and enzyme deactivation. A thermocycler instrument is used to raise and lower the temperature required for the different steps (82).

### 3.4.4   First strand cDNA synthesis procedure

Firstly, the RNA samples were diluted in DNase free water to achieve an appropriate concentration of RNA (200 ng/µl) for cDNA synthesis. High-Capacity RNA-to-cDNA (Thermo Fisher, 4387406) was used for cDNA synthesis. 10 µl of RT buffer mix and 1 µl of RT enzyme was added to 9 µl of diluted RNA sample. No enzyme was added to the -RT control. C1000 Thermal cycler (Bio-Rad) was used to run the RT reaction, under the following conditions: 37 °C for 60 minutes, 95 °C for 5 minutes, and 4 °C indefinitely. After cDNA synthesis, 180 µl of RNase free water was added to each sample, making the end cDNA concentration 1 ng/µl.

### 3.4.5 Principle of RT-qPCR

Polymerase chain reaction (PCR) is a method utilized to amplify specific DNA sequences. In RT qPCR, the amplification is monitored in real time using fluorescent DNA binding dyes or fluorescent probes. PCR involves three steps: denaturation, annealing and elongation. During the first step, denaturation, the sample is heated up to break the hydrogen bonds between the complementary DNA strands. In the next step, annealing, the sample is cooled down to allow the primers to bind to their complementary DNA strands. In the last step, elongation, the sample is heated up again and the DNA polymerase starts extending the complementary DNA strand. Taq DNA polymerase is most often used, due to its high thermostability. In qPCR, the fluorescent signal increases for each cycle as more PCR product is made, before reaching a plateau when reagents have been consumed. The cycle threshold (Ct) value is the cycle number in which the fluorescens signal is greater than the background signal (threshold). The threshold is sat in the region of exponential amplification (83), (84).

To observe relative gene expression in the samples, the ΔΔCt method, also known as the comparative CT method, can be utilized. To calculate the ΔΔCt, the samples are normalized against an endogenous control to adjust for variation in DNA content and quality. The endogenous control is a gene that is equally expressed in the different samples. The relative quantification (RQ) value represents the fold gene expression compared to a reference/control sample. The RQ value is calculated using the following equations (83).

$$1.\ \Delta Ct = Ct\ (gene\ of\ interest) - Ct\ (housekeeping\ gene)$$
$$2.\ \Delta\Delta Ct = \Delta Ct\ (sample) - \Delta Ct\ (reference\ sample)$$
$$3.\ Fold\ gene\ expression\ (RQ) = 2^{-\Delta\Delta Ct}$$

#### 3.4.5.1 Principle of TaqMan qPCR

In the TaqMan probe assay, a fluorogenic probe enable the detection of the PCR product. The probes consist of sequence specific oligonucleotides with a fluorescent reporter (R) dye at the 5' end and a quencher (Q) at the 3' end (Figure 3.2). When the reporter is in close proximity to the quencher, the energy from the light excitation of the reporter is transferred to the quencher in a phenomenon known as Fluorescence Resonance Energy Transfer (FRET). However, as the Taq polymerase starts to extend the complementary DNA strand, it cleaves the probe, and the reporter is separated from the quencher. The reporter will now emit detectable fluorescence (85).
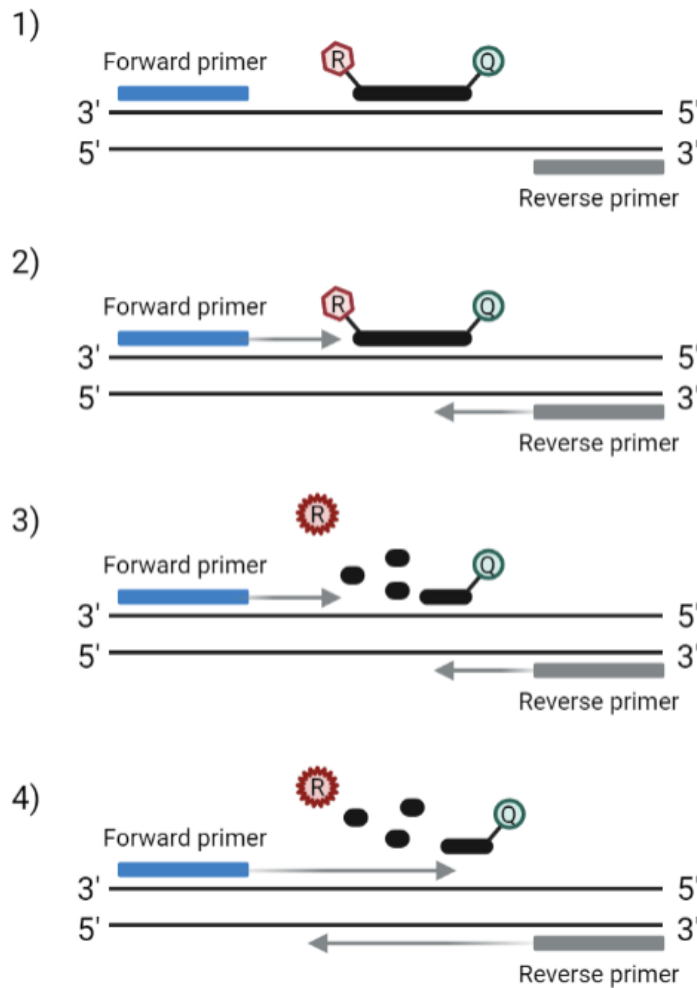
**Figure 3.2. Demonstration of the different steps in a TaqMan probe assay**. 1) The forward and reverse primer binds to their specific segments. As long as the TaqMan probe is intact, the reporter (R) is in close proximity to the quencher (Q), and the light emission from the reporter is quenched. 2) Taq polymerase starts to extend the complementary strand. 3) Taq polymerase extend the complementary DNA strand, cleaving the TaqMan probe, separating the reporter from the quencher. Light is emitted from the reporter. 4) Polymerization completed. Figure adapted from (83) and created with BioRender.com.

### 3.4.6 Procedure qPCR (TaqMan)

In this procedure, TaqMan™ Fast Advanced Master Mix (Thermo Fisher) was used. First, one reaction mix for every probe was made by combining TaqMan® Fast Advanced Master mix (2x), TaqMan probe (20x) and sterile ultrapure water (SIW). The volumes are listed in table 3.2. This reaction mix was then pipetted into a MicroAmp™ Fast Optical 96-well Reaction Plate before adding 5 ng of cDNA (1 ng/µl). The reaction plate was sealed with optical adhesive film and centrifuged at 1500 rpm for 2 minutes. StepOnePlus Real-Time PCR machine was used to perform the qPCR. The plate was run under the following conditions: holding stage of 20 seconds at 95 °C before 40 cycles with 95 °C for 1 second and 60 °C for 20 seconds. *GAPDH/Gapdh* and *ACTB*/*Actb* were used as endogenous controls. The

stock cell lines MOPC315.BM and JJN3 were used as reference samples and the fold gene expression was calculated using the ΔΔCt method on StepOne Software v2.3. TaqMan gene expression assay probes are produced by Thermo Fisher. The following probes were used: *B4galt1* (Mm00480752_m1), *St6gal1* (Mm00480752_m1), *Actb* (Mm00480752_m1), *Gapdh* (Mm99999915_g1), *B4GALT1* (Hs00155245_m1), *ST6GAL1* (Hs00949382_m1), *ACTB* (Hs03023943_g1), *GAPDH* (Hs99999905_m1).

**Table 3.2 PCR reagents and volumes**.

| Components | Volume per reaction (µl) |
|---|---|
| TaqMan®Fast Advanced Master Mix (2x) | 10 |
| TaqMan Probe | 1 |
| SIW | 4 |
| cDNA | 5 |
| Total volume per reaction | 20 |

## 3.5 Western blot

In this thesis, western blots were used to observe the protein expression of the two glycosyltransferases, B4GalT1 and ST6Gal1 in MOPC315.BM and JJN3 and to confirm or refute KD/OE of these transferases. Western blots were also performed to verify the presence of IgA in cell lysate and cell supernatant in relation to lectin blots.

### 3.5.1   Principe of western blot

Western blot is a method used to detect and semi-quantify a specific protein in a mixture of proteins. The method involves tree distinct steps: separating the proteins via gel electrophoresis, transferring the proteins to a membrane (blotting), and detection via protein specific antibodies (86). To access the proteins inside a cell, the cell membrane must be lysed. This is done by adding a lysis buffer, containing a detergent, salts, and a buffer. IGEPAL CA-630 is an example of a nonionic detergent, meaning it does not disrupt protein function.

When running a denatured polyacrylamide gel electrophoresis (PAGE), the proteins are separated based on their mass only. The negatively charged proteins are forced through the gel by an electrical current. A sample buffer containing an anionic detergent (SDS/LDS) is added to the sample to unfold the proteins and coat them in a negative charge. A reducing agent, most commonly DTT, is added to the sample buffer to disrupt disulfide bonds and

thereby contribute to the unfolding of the protein. Heating the sample after adding the sample buffer with DTT helps to accelerate protein denaturation.

A method commonly used for blotting is electrophoretic transfer, where the proteins move from the gel to a protein-binding membrane when an electrical field is applied. Blocking the membrane prior to antibody incubation is important to prevent the antibodies from binding nonspecifically to the membrane. The proteins are detected by using antigen specific antibodies. The detection method is commonly divided in two groups, direct and indirect detection. In direct detection, the antibody that binds specifically to the target protein is conjugated with an enzyme, that combined with the substrate produce a detectable signal. In the indirect methods, the primary antibody binds specifically to the target protein. The primary antibody is then detected by the secondary antibody, which is conjugated with an enzyme or fluorophore. Horseradish peroxidase (HRP) is an enzyme frequently used as a conjugate. When this enzyme reacts with a chemiluminescent substrate, light is produced as a byproduct (87), (88), (89).

### 3.5.2 Procedure of western blot

The cell pellets were resuspended in 40 µl of lysis buffer per $1 \times 10^6$ cells. The samples were mixed well and vortexed for 5-10 seconds before an incubation on ice for 20-30 minutes. To remove cell debris, the sample was centrifuged at 13 000 rpm for 15 minutes at 4 °C. After centrifugation, the supernatant was moved to a new tube. The content of the lysis buffer is listed in the following table (Table 3.4).

**Table 3.4. Lysis buffer used to lyse cells prior to western and lectin blots**

| |
|---|
| 1 % IGEPAL CA-630 (Sigma, MKCD3510) |
| 150 mM NaCl (Merck, 1.06404.1000 |
| 50 mM Tris-HCl (pH 7,5) (Sigma, T5941) |
| 10% Glycerol |
| 1 mM NaF (Sigma, 201154) |
| 2 mM $Na_3VO_4$ (BioVision, 9471-5) |
| Complete protease inhibitor (Roche, 11836170001) |
| Deionized water |

Sample buffer was made by mixing 1.0 M dithiothreitol (DTT) (AppliChem, A3668-0050) and NuPAGE $^{TM}$ LDS sample buffer (Thermo Fisher, NP0007). Sample buffer was added to

the protein sample in the ratio 1:4. The samples were then mixed by a short vortex before the proteins were denatured at 70 °C for 10 minutes. NuPAGE$^{TM}$ 4-12% Bis-Tris polyacrylamide gels (Thermo Fisher, NP0321, NP0322, WG1402) were used in XCell SureLock Mini-cell/XCell4 SureLock Midi-Cell systems with MOPC SDS running buffer (Thermo Fisher, NP0001) diluted in deionized water. PowerEase 500 (Invitrogen) was used as the power supply and the gel was run under the following conditions: 80 V for 30 minutes, 120 V for 30 minutes, and 150 V for 1 hour.

Blotting was performed utilizing iBlot™ 2 Gel Transfer Device (Thermo Fisher, IB21001) and iBlot™ 2 Transfer Stacks, nitrocellulose, mini/regular (Thermo Fisher, IB23002, IB23001). The blotting program P0 consists of three steps: 20 V for 1 minute, 23 V for 4 minutes and 25 V for 2 minutes. The membranes were blocked in 5% BSA (Sigma, A7906) in 0.1% TBS-T or 5% non-fat dry milk (DFDM) (Normilk, 127007) in 0.1% TBS-T, depending on the manufacturer's recommendations and our own testing. After blocking for one hour, the membranes were incubated with the primary antibody overnight in 4 °C (for indirect detection). The next day, the membranes were washed for 3×5 minutes in 0.1% TBS-T and thereafter incubated with the secondary antibody conjugated with HPR (listed in Appendix II). After one hour the membranes were washed (5×5 minutes), before incubation with SuperSignal$^{TM}$ (Thermo Fisher, 34579) for 2-3 minutes. The membranes were then imaged using LI-COR odyssey FC imager and Image Studio. When using a direct detection method, the membranes were incubated with the antibody for one hour, followed by washing (5×5 minutes), and imaging. The primary antibodies used for western blots are listed in the following table (Table 3.5).

**Table 3.5. List of antibodies used for western blots.** Antibodies marked with * is diluted in 5% non-fat dry milk, while the rest of the antibodies are diluted in 5% bovine serum albumin.

| Antibody | Source | Manufacturer | Catalog number | Reactivity | Dilution |
|---|---|---|---|---|---|
| B4GALT1* | Rabbit | Affinity Sciences | DF3839 | Mouse, (Human) | 1:1000 |
| B4GALT1 | Goat | R&D Systems | AF3609 | Human | 1:2000 |
| ST6GAL1 | Goat | R&D Systems | AF5924 | Human, Mouse | 1:200 |
| IGHA1 | Rabbit | ThermoFisher | PA5-86579 | Human, (Mouse) | 1:500 |
| Anti-IgA | Goat | Abcam | Ab97235 | Mouse | 1:5000 |
| GAPDH | Mouse | Abcam | Ab8245 | Human, Mouse | 1:30 000 |
| Beta-actin | Rabbit | Cell Signaling T. | 4967S | Human, Mouse | 1:1000 |
| IgG4* | Mouse | Merck | MAB1312 | Human | 1:1000 |

## 3.6 Lectin blot

Lectin blots were used to observe the glycosylation of both proteins inside the cells (cell lysate), and proteins secreted by the cells (supernatant/serum). The aim was to use lectin blots to investigate whether there was an increase/decrease in galactosylation and sialylation of proteins in ST6Gal1/B4GalT1 MOPC315.BM KD clones and JJN3 OE cells.

### 3.6.1    Principe of lectin blot

Lectin blot is a method used to detect the glycosylation of proteins. The lectin blot method is similar to western blotting. Only the detection method differs from a standard western blot procedure. The proteins are denatured, separated, and blotted onto a membrane following the same principles as described in 3.5.1. When performing a lectin blot procedure, it is important to not use a blocking substance (e.g., dry milk) containing the carbohydrate of interest, as this might increase background interference. After blocking, the membrane is incubated with the biotinylated lectin. When the lectins have bound to their specific carbohydrate, the avidin-biotin complex reagent is added. The biotin conjugated to the lectin will bind one streptavidin molecule, which further can bind three more biotin molecules conjugated with HRP. When adding the substrate, the chemical reaction occurring causes the emission of light. The following figure (Figure 3.3) demonstrate the detection principle for lectin blot when utilizing biotinylated lectin.
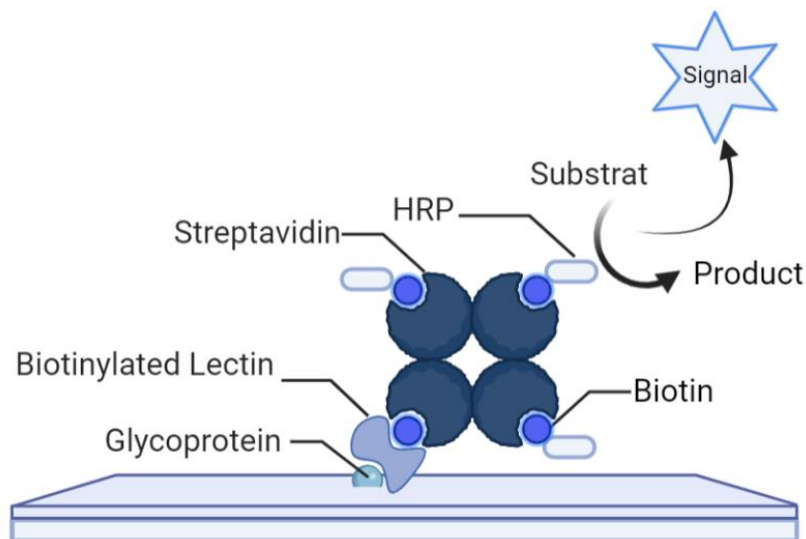


**Figure 3.3. Demonstration of how biotinylated lectins can be used to detect specific sugars.** The biotinylated lectin binds to a specific glycoprotein. The biotin conjugated to the lectin will bind one streptavidin molecule, which further binds three more biotin molecules conjugated with HRP. The chemical reaction occurring when adding the substrate causes the emission of light. HRP = Horseradish peroxidase. Figure created with BioRender.com.

### 3.6.2 Procedure for lectin blot

Lectin blots follow the same procedure as western blots up until the blocking. Additionally, total protein concentration of the lysate/serum was measured using Bradford reagent (Bio-Rad, 5000205). Absorbance was measured at 595 nm using iMark Microplate Absorbance Reader (BioRad). Protein concentration was calculated from the standard curve, made from a two-fold dilution series of Bovine Serum Albumin (BSA) (Thermo Fisher, 23235). The samples protein concentration was made equal by diluting the samples in lysis buffer. In some experiments, Ponceau S (Sigma, P 7170) was used as a total protein staining and loading control. The membrane was stained with Ponceau S for 5-10 seconds, before being rinsed in water and imaged using LI-COR odyssey FC imager and Image studio. After imaging, the membrane was washed in 0.1% TBS-T.

Blocking was performed for 30 minutes, using Carbo-Free Blocking Solution (CFBS) (Vector, ZF1107). After blocking, the membrane was incubated with the biotinylated lectins for 30 minutes. The lectins used were Sambucus Nigra Lectin (SNA) (Vector, B-1305-2), Erythrina Cristagalli Lectin (ECA) (Vector, B-1145-5) and Lens Culinaris Agglutinin (LCA) (Vector, B-1045-5). The lectins were diluted 1:1000 in DPBS. After incubation with the lectins, the membranes were washed for 3×5 minutes in 0.1% TBS-T before incubation with VECTASTAIN®ELITE®PK-6100 ABC kit Peroxidase (HRP) (Vector, PK-6100) diluted in CFBS. After 30 minutes of incubation, the membranes were washed for 5×5 minutes in 0.1% TBS-T before a short incubation (5-10 seconds) with Pierce $^{TM}$ ECL Western Blotting Substrate (Thermo Fisher, 32109). The membranes were imaged using LI-COR odyssey FC imager and Image Studio.

## 3.7 Cell Titer Glo (CTG)

In this thesis, Cell Titer Glo was used to analyze cell viability in MOPC315.BM stimulated with puromycin.

### 3.7.1 Principe of Cell Titer Glo

CellTiter-Glo® Luminescent Cell Viability Assay quantitates the amount of ATP in a culture of cells. ATP production in a culture indicates the presence of metabolically active cells. When a cell dies, the ATP production rapidly decreases, as cell metabolism is shut down and ATP is degraded by ATPases. The CTG reagent contains ATPase inhibitors to ensure that

ATP is not degraded upon cell lysis. The enzyme luciferase, catalyze mono oxygenation of the substrate, luciferin. Luminescence is a biproduct in this reaction and ATP and $Mg^{2+}$ are required co-factors (Figure 3.4). The luminescent signal produced in this reaction is proportional to the amount of ATP present in the sample. The amount of ATP present in a cell culture is normally directly proportional to the number of live cells. However, factors that change the physiology of the cell can change the ATP content (e.g., oxygen depletion). This will disturb the relationship between luminescent signal and the number of cells (90), (91).
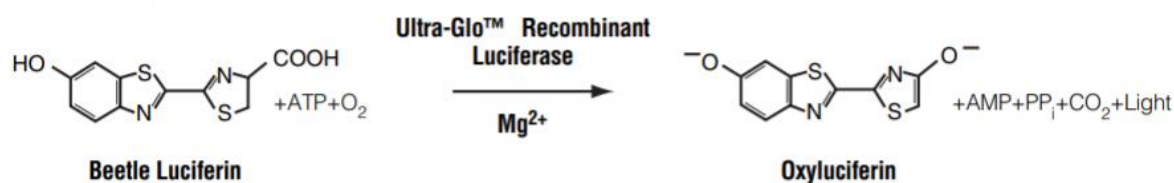


**Figure 3.4. Luciferase reaction.** The chemical reaction occurring where the enzyme luciferase, catalyze mono oxygenation of the substrate, luciferin. ATP and Mg2+ are required co-factors in this reaction. Illustration taken from manufacturers protocol (90).

### 3.7.2  Procedure for Cell Titer Glo

When analyzing the puromycin sensitivity in MOPC315.BM, 5.000 cells were seeded out per well (96 well optical plate) in different concentrations of puromycin, ranging from $0 – 5$ µg/ml. The plate was incubated for 24 hours (37 °C, 5% $CO_2$). The reagent CellTiter-Glo® (Promega, G92413) was prepared in advance by mixing CellTiter-Glo substrate and CellTiter-Glo buffer. The plates were incubated in room temperature for about 20 minutes before adding 70 µl of the Cell-Titer-Glo® reagent. Thereafter, the plates were put on a shaker for 2 minutes, followed by an incubation in room temperature for 10 minutes. The plate was light protected during shaking and incubation. Luminescence was measured using Victor 1420 multilabel counter and Wallac software.

### 3.8 Flow cytometry

In this thesis, flow cytometry was used to analyze puromycin sensitivity in MOPC315.BM and cell viability in ST6Gal1/B4GalT1 MOPC315.BM KD and ST6Gal1/B4GalT1 JJN3 OE. In addition, flow cytometry was used to analyze the percentage of eGFP positive cells in the eGFP positive control used in the transduction of MOPC315.BM and JJN3 with ORF expression plasmid.

### 3.8.1 Principe of flow cytometry

In flow cytometry, the chemical and physical properties of a cell or particle is analyzed. A suspension of cells/particles is led through the flow chamber, where a sheath fluid forces the cells/particles to form a single line, passing the laser(s) one by one. This technique is called hydrodynamic focusing and is a prerequisite for being able to analyze cells individually. When a cell passes the laser, the scattered light is measured in two angles. Forward scatter (FSC) detects scatter along the path of the laser and indicate the relative size of the cell. Side scatter (SSC) is measured at a 90° angle of the laser beam and indicate the shape and internal complexity of the cell (granulation). In addition, cells are commonly stained with fluorescent dyes (e.g., Propidium Iodine, PI) or antibody-conjugated fluorophores (e.g., Fluorescin isothiocyanate, FITC) that emits light (emission spectrum). Modern flow cytometers usually have multiple lasers and detectors, that enables the detection of several fluorophores at the same time (92), (93).

#### 3.8.1.1 Annexin V - FITC

Annexin V is a protein that binds to phospholipid phosphatidylserine (PS). In healthy cells, PS is located on the inner/cytoplasmic surface of the cell membrane. However, as a cell goes into apoptosis, the cell membrane is structurally changed, and PS is translocated to the outer side of the cell membrane (Figure 3.5). This allows Annexin V to bind to PS. The Annexin V used in this thesis is labeled with the fluorophore FITC. FITC has an emission maximum at approximately 525 nm (94), (95).
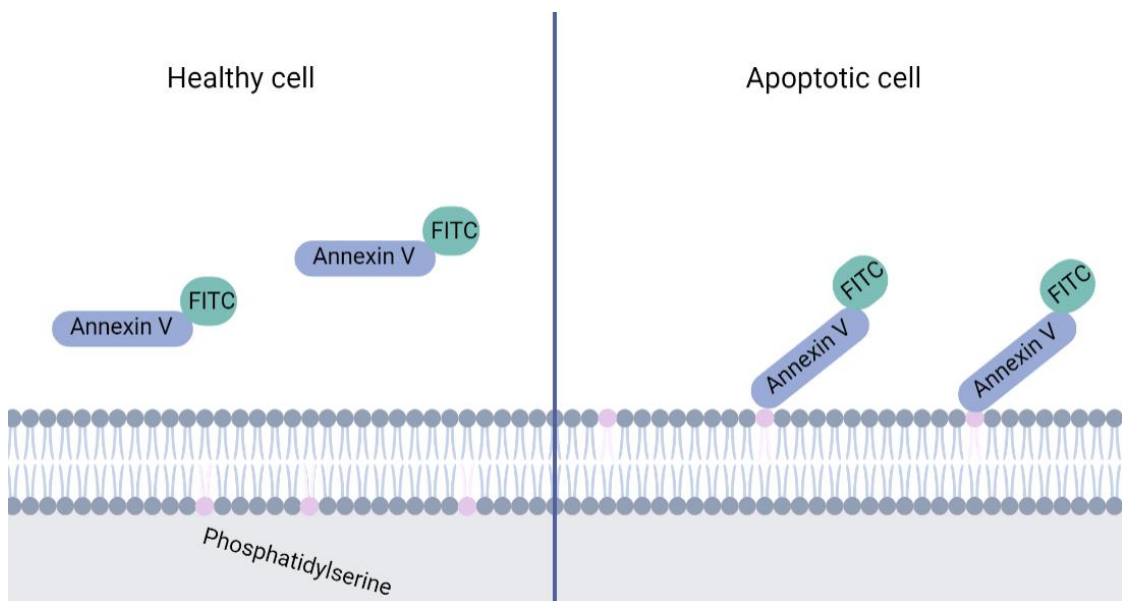


**Figure 3.5. Annexin V-FITC staining.** Phospholipid phosphatidylserines translocate to the outer side of the cell membrane in apoptotic cells, making it accessible for binding to Annexin V. Figure created with BioRender.com.

### 3.8.1.2 Propidium Iodine (PI)

PI is a fluorescent dye used to stain dead cells. PI binds to DNA by intercalating between the bases in the DNA strand. When a cell is healthy, the cell membrane is intact, and PI cannot enter the cell and bind to DNA. However, during necrosis or late-stage apoptosis the permeability of the membrane is increased, allowing PI to enter the cell. In solution PI has an emission maximum of 636 nm, when bound to DNA, the fluorescens emission maximum shifts to approximately 617 nm (96). The following figure demonstrate how cells place in a scatter plot when stained with Annexin V-FITC and PI (Figure 3.6).
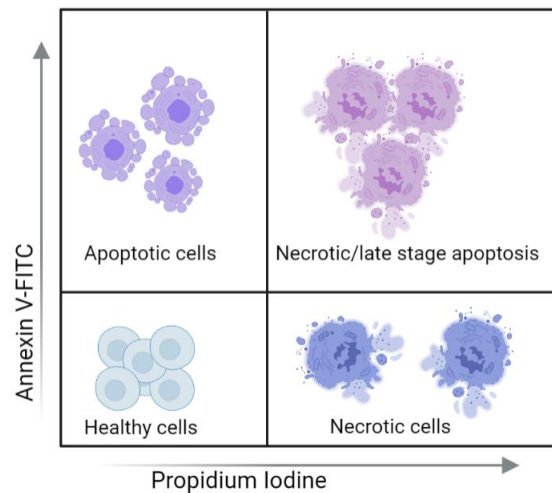


**Figure 3.6. Demonstration of how cells place in a scatter plots when stained with Annexin V-FITC and Propidium Iodine (PI).** The scales are logarithmic and the Annexin V-FITC signal is placed on the Y-axis, while the PI signal is placed on the X-axis. Figure created with BioRender.com.

### 3.8.2 Procedure for flow cytometry (AnnexinV-FITC/PI staining)

When analyzing the puromycin sensitivity in MOPC315.BM, 200 000 cells were seeded per well and stimulated with different puromycin concentrations (0 - 5 µg/ml) for 24 hours. When analyzing cell survival in MOPC315.BM and JJN3 ST6Gal1/B4GalT1 KD/OE cells, 400 000 cells were harvested. During the whole procedure, the cells were kept on ice. The cells were transferred to flow tubes and centrifuged for 5 minutes, 1500 rpm, 4 °C. The supernatant was discarded, and the cells were washed in ice cold DPBS and centrifuged for 5 minutes, 1500 rpm, 4 °C. The supernatant was discarded once again. 300 µl of Binding buffer (Tau Technologies, BB19002) + 0,25 µl Annexin V FITC (Tau Technologies, FI19016) was added to each sample followed by an incubation for one hour, on ice and protected from light. After the incubation, 50 µl of binding buffer + 2 µl of PI (Invitrogen, P16063) was added to each

sample. The samples were analyzed using BD LSRII flow cytometer (BD Bioscience) and BD FACSDiva™ software.

## 3.9 M315 protein treated with neuraminidase

To investigate whether terminal sialic acid residues inhibit the binding of lectin ECA to galactose, purified M315 protein (from B. Bogen, Oslo University Hospital) was treated with the enzyme neuraminidase. M315 protein is the M-component produced by MOPC315.BM cells and consists of IgA (λ2 light chain). Neuraminidases are a group of enzymes that cleave the glycosidic linkages of neuraminic acids i.e., sialic acid (Figure 3.7). M315 protein was diluted in GlycoBuffer 1 (BioLabs, B1727S) before adding 40 U of α 2-3,6,8,9 Neuraminidase A (BioLabs, P0722L). Two controls were also included, one control with M315 protein diluted in GlycoBuffer (no enzyme) and one control with only GlycoBuffer and enzyme (no M315 protein). The samples were incubated 24 hours before galactose and sialic acid was detected by lectin blots.



**Figure 3.7. Demonstration how neuraminidase cleaves the glycosidic linkage between galactose and sialic acid**. When sialic acid residues are removed, galactose is accessible for binding of lectin ECA. Figure created with BioRender.com.

## 3.10    Vk*myc 12653

Vk*myc is a MM mouse model based on dysregulation of the *MYC* locus. Rearrangements in this locus is the most abundant genetical abnormality in human MM and is associated with the progression of monoclonal gammopathy. Vk*myc cells are dependent on the microenvironment of the BM and do not grow *in vitro* but are maintained by serial transplantation into mice (C57Bl/6). When injected into mice, the mice develop MM with a high secretion of monoclonal Igs (97).

Our research group was interested in learning more about the glycosylation of these Igs. Therefore, serum from a mouse injected with Vk*myc 12653 cells, and serum from a negative control mouse was collected at euthanasia. The BM of the mice injected with Vk*myc consisted of about 20% tumor cells. The serum was analyzed by lectin and western blots. In

addition, IgG was purified from both serum samples utilizing Protein G HP SpinTrap (Sigma, 28903134), following the manufacturer's procedure. The SpinTrap is packed with protein G Sepharose, which has a high affinity for the Fc region of IgG. The binding capacity of protein G Sepharose is determined by the pH of the solution. A binding buffer (20 mM sodium phosphate) with pH 7.0 is added for optimal binding of the antibody. When eluting the antibody, an elution buffer (0.1 M glycine-HCl) with pH 2.5-3.0 is added. The purified IgG is quickly neutralized by adding neutralization buffer (1M Tris-HCl) with pH 9.0 to the collection tube.

### 3.11    Statistical analysis

Statistical analyses were performed in GraphPad Prism 9. One-way ANOVA and Šídák's multiple comparisons test were used to compare different groups.

# 4. Results

Previous research has shown that the monoclonal Igs of MM patients with bone disease have reduced IgG-Fc sialylation and galactosylation. Our group have previously analyzed the expression of glycosyltransferases in myeloma cells from patients with bone disease and without bone disease. The glycosyltransferases *ST6GAL1* and *B4GALT1* were found to be significantly less expressed in patients with BD. Thus, reduced Ig galactosylation and sialylation may be caused by reduced expression of glycosyltransferases in myeloma cells. To follow up this research, we wanted to establish MM cell lines with modified glycosyltransferases, to further understand how glycosylation affects MM bone disease.

The results are divided in five parts. The results from the KD and OE of ST6Gal1/B4GalT1 in MOPC315.BM cells and the OE of ST6Gal1/B4GalT1 in JJN3 cells are presented in the first three parts. Results on whether terminal sialic acid residues inhibit the binding of lectin ECA to galactose are presented in part four. In part five, results regarding glycosylation of IgG in Vk*myc 12653 are presented.

## 4.1 MOPC315.BM ST6Gal1/B4GalT1 knockdown

Here, results regarding the testing of puromycin sensitivity in MOPC315.BM, knockdown of ST6Gal1/B4GalT1 in MOPC315.BM and the potential effects of this knockdown regarding cell growth and viability are presented.

### 4.1.1   Testing puromycin sensitivity in MOPC315.BM

After the KD of ST6Gal1/B4GalT1 in MOPC315.BM, by lentiviral transduction (shRNA), the cells were cultivated in selection media (puromycin) to promote the growth of only the cells that had implemented the expression construct in their genome. CTG assay and flow cytometry (Annexin V-FITC/PI staining) was utilized to find the optimal concentration of puromycin in the selection medium. An optimal concentration would be the point in which the cells without the resistance gene die. The results from the CTG assay (Figure 4.1 A) indicate a clear decrease in the number of live cells at a puromycin concentration of 1.5 µg/ml. At a puromycin concentration of about 4 µg/ml, almost all cells are dead. Similar results are seen in the Annexin V-FITC/PI staining analyzed by flow cytometry (Figure 4.1 B). The scatter plots from a two-dimensional plot of Annexin V-FITC (Y-axis) against PI (X-axis) staining show how the cells place in the plot, at different puromycin concentrations (Figure 4.1 C). At lower puromycin concentrations, a population of apoptotic cells locate in Q1. Late stage

apoptotic and necrotic cells located in Q2, are considered as dead, and increase with increasing puromycin concentration. Based on these data, 4 µg/ml puromycin appears to be an appropriate concentration for the selection media.
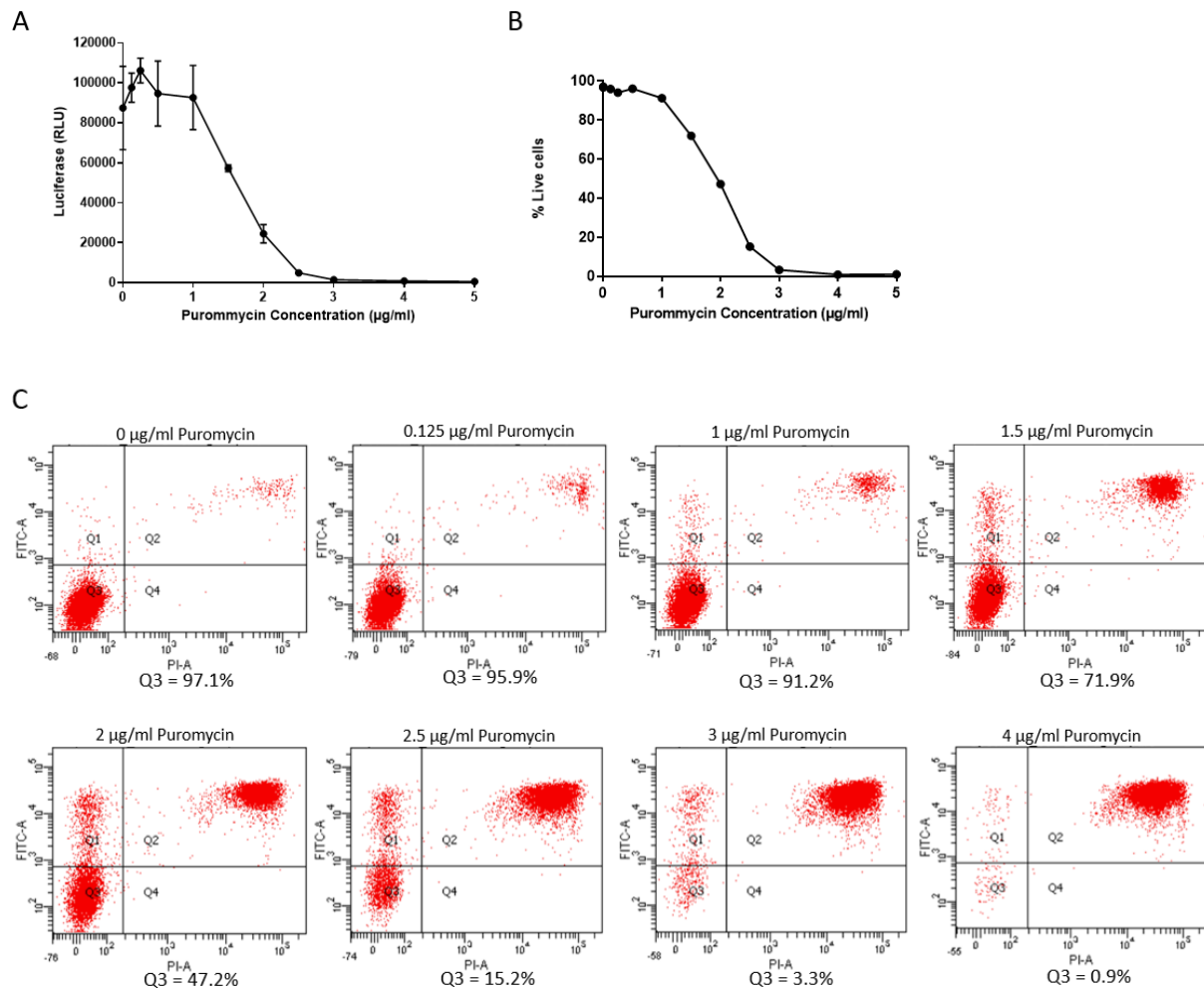


**Figure 4.1. Testing the puromycin sensitivity in MOPC315.BM utilizing two different methods**. A: CellTiter-Glo® Luminescent is used to measure cell viability. 5.000 cells per well were incubated with 0 to 5 µg/ml puromycin for 24 hrs. The experiment was performed three times, testing different cell concentrations. The results are plotted as mean of three technical replicates with error bars (± SD) from an optimized experiment. B: Cell viability measured by flow cytometry with Annexin V-FITC and PI staining. 200.000 cells were seeded out per well and incubated for 24 hrs. Different concentrations of puromycin, ranging from 0 to 5 µg/ml, was added to the wells. The results present percentage of live cells (Q3 in scatter plot). The experiment was performed three times, seeding out different concentrations of cells. The results presented in this figure show the results from one representative experiment. C: Scatter plots (FITC-A on the Y-axis and PI-A on the X-axis) for each concentration of puromycin. Q3 represent live cell. Apoptotic cells will locate in Q1, necrotic cells locate in Q4 and dead cells (necrotic or late-stage apoptosis) will locate in Q2.

### 4.1.2 Successful knockdown of the glycosyltransferases ST6Gal/B4GalT1 in MOPC315.BM at gene and protein level

The gene expression of *St6gal1/B4galt1* in MOPC315.BM ST6Gal1/B4GalT1 KD was analyzed by qPCR (Figure 4.2 A) to investigate if the attempt to knock down these transferases was successful. These results show that the gene expression of *St6gal1* in St6Gal1 KD is nearly halved (41% KD) compared to *St6gal1* expression in the MOPC315.BM control. The gene expression of *B4galt1* in B4Galt1 KD is also halved (58% KD) compared to the gene expression of *B4galt1* in the MOPC315.BM control. These promising results lead to the process of cloning by limiting dilution in attempt to obtain single cell cultures. The cloning resulted in 1. selection of 11 control clones, named MC 1-11, 26 ST6Gal1 KD clones, named ST6 1-26 and 31 B4GalT1 KD clones, named MB 1-31. The relative gene expression of *St6gal1* and *B4galt1* was analyzed (qPCR) in all these clones (see appendix III). Based on the results from the qPCR, 6 MST and 5 MB clones with the lowest *St6gal1/B4galt1* expression were chosen for further analysis in addition to 3 MC clones with gene expression of *St6gal1/b4galt1* most similar to MOPC315.BM wild type. A second qPCR of the selected clones was performed to confirm the results from the previous qPCR (Figure 4.2 B).

Protein expression was analyzed by western blots with protein quantification. The western blot (Figure 4.2 C) shows a clear decrease (68-99%) in the amount of ST6Gal1 in MST clones compared to the MC clones and MOPC315.BM. There is also a reduction in the amount of B4GalT1 (0-64% KD) in the MB clones, although this reduction is not that evident (Figure 4.3 D). The clones MST5, MST23, MB11, MB25 shows the most promising results in terms of KD of the glycosyltransferases at both gene and protein level. These clones along with the control clones MC2 and MC4 were chosen for further analysis.
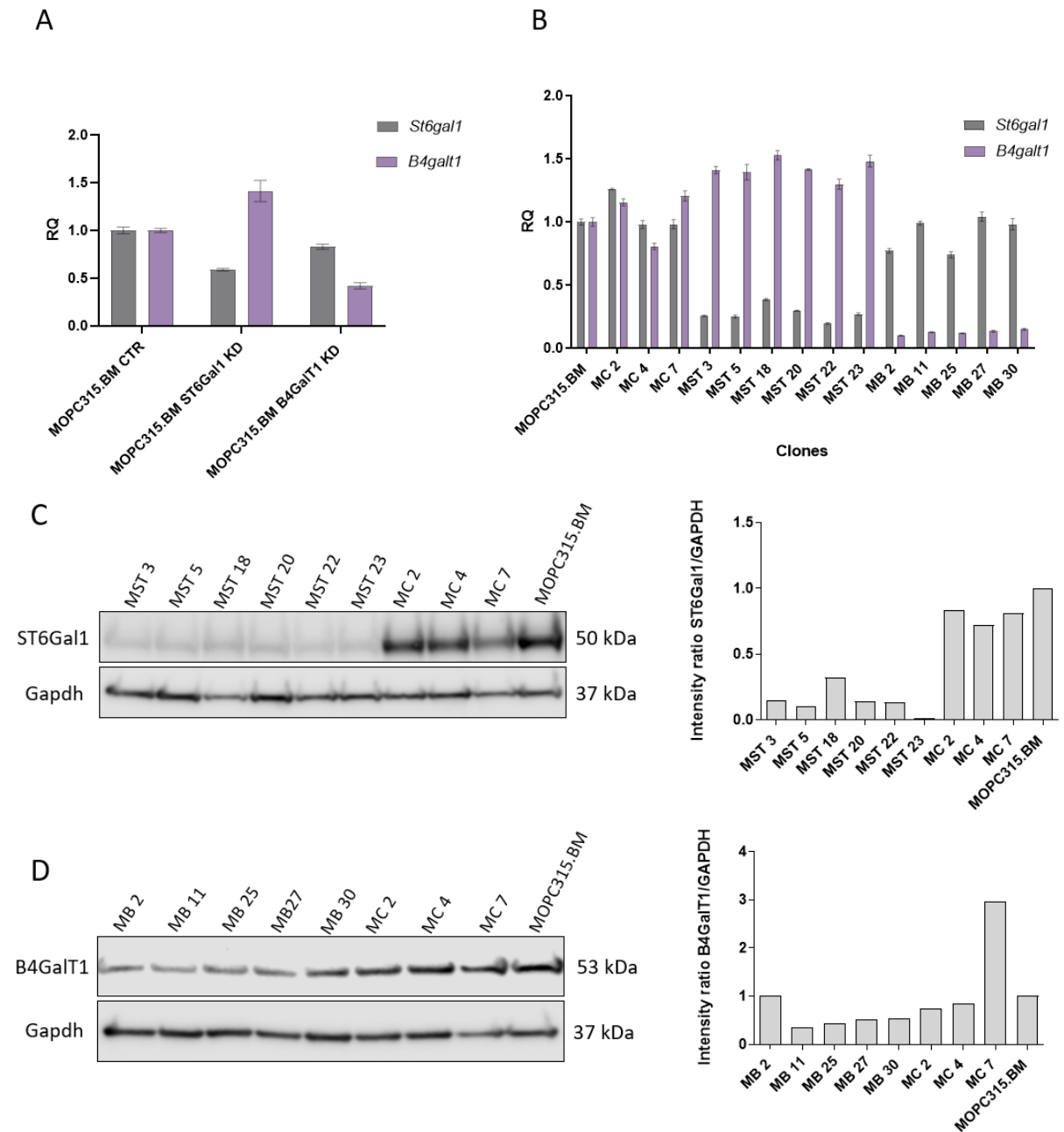
**Figure 4.2**. **Gene and protein expression of the glycosyltransferases ST6Gal1 and B4GalT1 in MOPC315.BM. ST6Gal1/B4GalT1 KD**. A: The gene expression of *St6gal1* and *B4galt1* in MOPC315.BM ST6Gal1 KD and B4GalT1 KD cells is analyzed by qPCR before cloning. MOPC315.BM CTR is used as "reference sample" and *Gapdh* is the endogenous control. B: Second qPCR of a limited number of selected clones; 3 control clones (MC 2, 4, 7), 5 ST6Gal1 KD clones (MST 3, 5, 18, 20, 22 and 23) and 5 B4GalT1 KD clones (MB 2, 11, 25, 27, 30). MOPC315.BM is used as reference sample and *Gapdh* is the endogenous control. RQ is calculated using the comparative CT method and bars represent mean $\pm$ SD from two technical replicates. C-D: Protein expression of the selected ST6Gal1 KD or B4GalT1 KD clones analyzed by western blot. Bars represent quantification of the signal detected of each sample relative to the signal detected in MOPC315.BM. Gapdh is used as lading control. (MST = St6Gal1 KD clones, MB = B4GalT1 KD clones, MC = control clones).

### 4.1.3 No difference in cell viability and doubling time in ST6Gal1/B4GalT1 MOPC315.BM knockdown clones

To investigate if the selected clones divide at the same rate as untreated MOPC315.BM, the doubling time was calculated based on four different cell counts at different times (Figure 4.3 A). The doubling time range from 14,2 hours to 16,7 hours. There is no significant difference in the doubling time between the individual clones and MOPC315.BM/control clones. To investigate whether KD of ST6Gal1/B4GalT1 influence the cell viability, the selected clones were analyzed by flow cytometry (annexin V-FITC/PI staining) (Figure 4.3 B). The cell viability ranges from 97.1% - 98.5% and appears to be similar between the clones and MOPC315.BM. The results presented in figure 4.3 indicate that the KD of ST6Gal1/B4GalT1 in MOPC315.BM does not affect the doubling time or the cell viability of these cells.

A
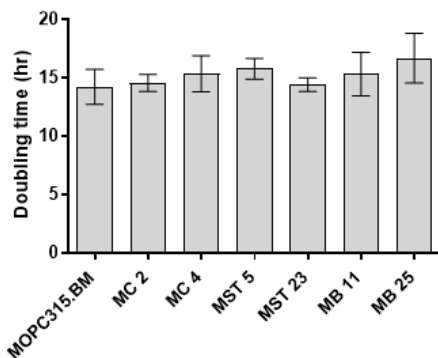


B
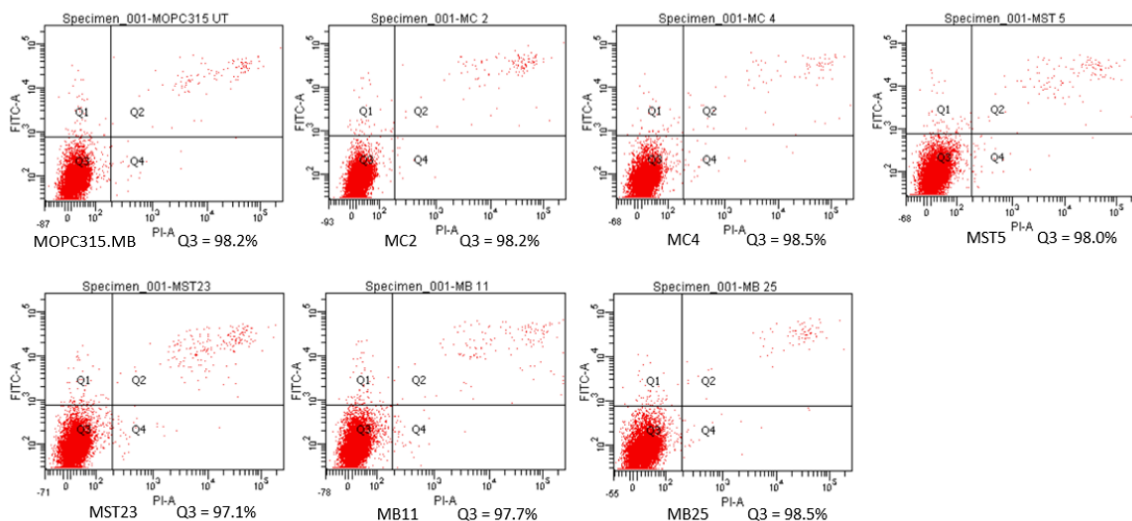


**Figure 4.3. Testing cell growth (doubling time) and cell viability in MOPC315.BM ST6Gal1/B4GalT1 KD clones**. A: The doubling time is calculated as described (2.1.4), from four individual cell counts, at different times. The results are plotted as mean of four replicates $\pm$ SD. B: Cell viability in the selected MOPC315.BM clones are measured using Annexin/PI staining and flow cytometry. Live cells are detected in the Q3 section of the scatter plot. (MST = St6Gal1 KD clones, MB = B4GalT1 KD clones, MC = control clones)

### 4.1.4 Non conclusive results regarding galactosylation and sialylation of proteins in ST6Gal1- or B4GalT1 MOPC315.BM knockdown clones

Lectins blots were used to investigate whether the decreased expression of the glycosyltransferases cause a decrease in galactosylation/sialylation of proteins. The lectin blot from cell lysate, incubated with the lectin ECA, which binds to galactose (Figure 4.4 A) show no apparent differences in the galactosylation of proteins when comparing the ST6Gal1/B4GalT1 KD clones to the control clones and MOPC315.BM. The lectin blot from cell lysate, incubated with the lectin SNA, which binds to sialic acid (Figure 4.4 B) show no sign of a reduction in sialylated proteins in the ST6Gal1/B4GalT1 KD clones compared to control clones and MOPC315.BM.

The blots showed in figure 4.4 are total cell lysates and therefore show all proteins in the cell that are galactosylated (Figure 4.4 A) or sialylated (Figure 4.4 B). We wanted to investigate glycosylation of IgA heavy chain specifically and tried to purify IgA from the cell lysate, but without any success. Another option was to harvest the supernatant, as MOPC315.BM secrete IgA. The harvested supernatant from the clones and MOPC315.BM was analyzed by lectin blot (SNA) and a western blot (detecting IgA) (Figure 4.4 C). Purified and concentrated IgA λ2 light chain (M315 protein) from MOPC315.BM cell supernatant, (a gift from Bogens research group in Oslo) was used as a control. The experiment was repeated three times (biological replicates) and the glycosylation was quantified (Figure 4.4 D). An antibody against IgA heavy chain was used to confirm the presence of IgA in the supernatant. The amount of sialic acid in the clones is relative to the amount of sialic acid in MOPC315.BM (Figure 4.4 D). There is no significant difference in IgA-Fc sialylation in ST6Gal1 KD clone MST5 or B4GalT1 KD clone MB11 compared to MOPC315.BM or the control clone MC2.

When attempting to detect galactosylation in secreted IgAs with the use of lectin ECA, no bonds were detected. This discovery led us to believe that lectin ECA might be inhibited from binding to the glycan if terminal sialic acid residues are present on the structure.
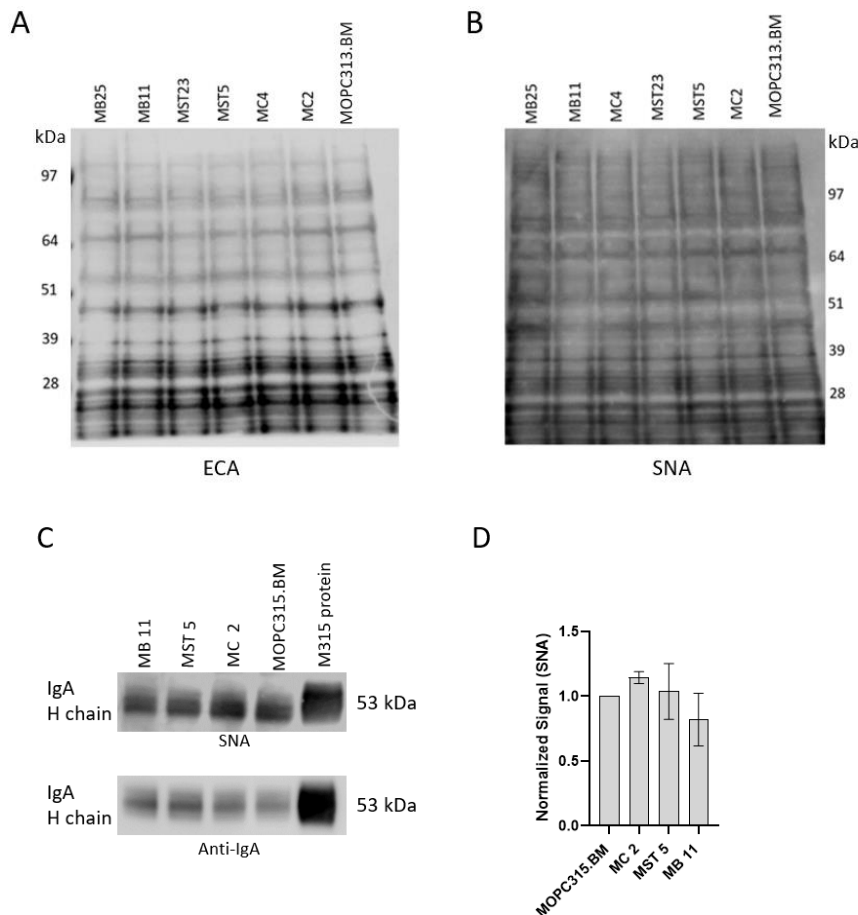
**Figure 4.4**. **Lectin blot analysis of MOPC315.BM ST6Gal1/B4GalT1 KD clones to detect glycosylation of proteins.** A: Lectin blot of total cell lysate incubated with ECA to detect galactosylated proteins and B: Lectin blot of total cell lysate incubated with SNA to detect sialylated proteins. C. An equal number of MOPC315.BM, ST6Gal1 KD (MST5), B4GalT1 KD (MB11) and control (MC2) was seeded out in medium (500 000 per ml) without FBS. The supernatant was harvested after 24 hours and analyzed by western blot (detecting IgA) and Lectin blot (SNA.) M315 protein is purified and concentrated M protein i.e., IgA ($\lambda$2 light chain) from MOPC315.BM cell supernatant. D: Lectin blot (SNA) in C. was quantified and the amount of sialic acid in the clones are relative to the amount of sialic acid in untreated MOPC315.BM. (FBS = Fetal bovine serum, MST = St6Gal1 KD, MB = B4GalT1 KD clones, MC = control clones). Bars represent three biological replicates (n=3) (mean $\pm$ SD).

## 4.2 No overexpression of the glycosyltransferases ST6Gal1 or B4GalT1 in MOPC315.BM after lentiviral transduction

The attempt to overexpress St6Gal1 and B4galt1 in MOPC315.BM via lentiviral transduction did not succeed. Figure 4.5 present the results from analysis performed on MOPC315.BM ST6Gal1/B4GalT1 OE. A lentiviral transfer vector that expresses the eGFP protein was used as positive control. The amount of eGFP positive cells was analyzed by flow cytometry (Figure 4.5 A) and give an estimate of the amount of MOPC315.BM cells infected with the

lentiviruses. The histogram shows the number of cells with different intensities of the GFP signal. Cells with higher intensity than the negative control cells, locate in the P2 region of the histogram and are considered eGFP positive. MOPC315.BM cells were transduced at two virus dilutions (1:10 and 1:2) and both show a low amount (approximately 7% and 20%) of eGFP positive cells. Untreated MOPC315.BM was used as negative control.

Relative gene expression of *St6gal1 or B4galt1* in MOPC315.BM St6Gal or B4GalT1 OE cells was analyzed by qPCR (Figure 4.4 B). The qPCR results show no overexpression of either *St6gal1* or *B4galt1*. To make sure that the gene sequence of the ORF expressing plasmids used to overexpress ST6Gal1 and B4GalT1 was compatible with the qPCR primers, a PCR with the purified plasmids was performed (Figure 4.4 C). The plasmid DNA was diluted1:500 prior to analyzes. There is sequence compatibility between the *St6gal1* expressing plasmid and the *St6gal1* primer, indicated by the low CT values. Low CT values are also seen in the PCR with the *B4galt1* expressing plasmid when utilizing the *B4galt1* primer. The empty plasmids, which are used in the transduction of the control cells, are not detected by the *St6gal1* or the *B4galt1* primers



| Sample/plasmid | CT Mean | |
| | *St6gal1* | *B4galt1* |
| --- | --- | --- |
| *Sample/plasmid* | ST6GAL1 | B4GALT1 |
| *MOPC315.BM* | 25.73 | 26.61 |
| *Ex-neg-LV105Empty 1:500* | Undetermined | Undetermined |
| *Ex-mm05221-LV105 St6gal1 1:500* | 15.95 | Undetermined |
| *Ex-mm02717-LV105 B4galt1 1:500* | Undetermined | 14.96 |
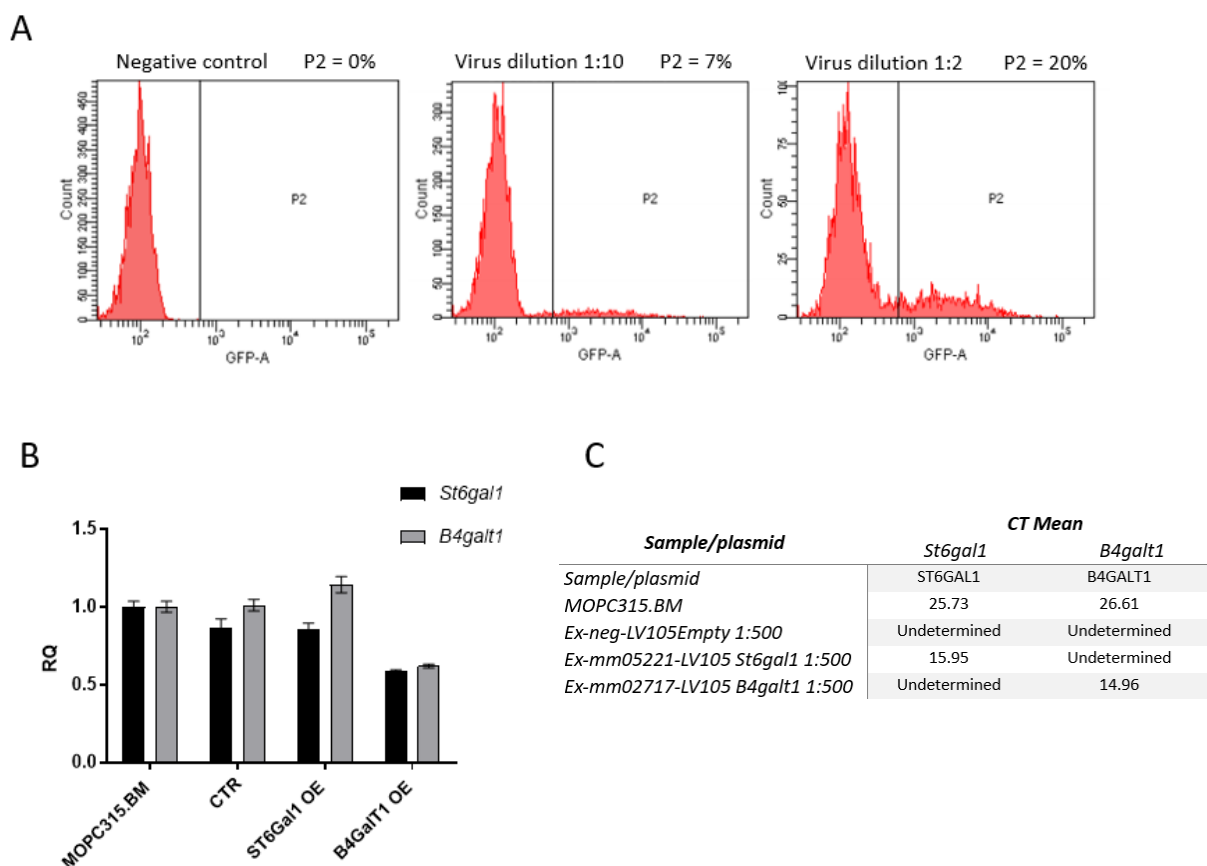
**Figure 4.5. Analysis performed on MOPC315.BM after attempting to overexpress ST6Gal1 and B4GalT1 via lentiviral transduction**. A: Histogram of MOPC315.BM transduced with eGFP expressing vector at two different virus dilutions. Cells in P2 are calculated as eGFP positive. Untreated MOPC315.BM was used as negative control. B: qPCR of MOPC315.BM ST6Gal1 and B4GalT1 OE. MOPC315.BM is used as reference sample and beta-actin as endogenous control. RQ is calculated using the comparative CT method. Bars represent the mean ± SD and is calculated from two technical replicates. C: qPCR of the MOPC315.BM cDNA and the purified plasmids used in the transduction of MOPC315.BM; Ex-neg-LV105 Empty (control vector), Ex-mm05221-LV105 St6gal1 (vector expressing ST6gal1) and Ex-mm02717-LV105 B4galt1 (vector expressing B4galt1).

## 4.3 JJN3 ST6Gal1/B4GalT1 overexpression

Here the experiments performed to investigate the overexpression of ST6Gal1 and B4GalT1 in JJN3 cells and potential effects regarding cell growth and viability are presented.

### 4.3.1 High amount of eGFP positive JJN3 cells, transduced with eGFP expressing vector

A lentiviral transfer vector that expresses the eGFP protein was used as positive control for transduction of JJN3 cells. The amount of eGFP positive cells were analyzed by flow cytometry (Figure 4.6) and give an estimate of the amount of JJN3 cells infected with the lentiviruses. Untreated JJN3 cells were used as negative control and cells with higher intensity than the negative control cells, locate in the P2 region of the histogram and are considered eGFP positive. JJN3 cells transduced with eGFP at virus dilution 1:10 gives approximately 15% positive cells. A virus dilution of 1:2 give a high amount (97.8%) of eGFP positive cells.
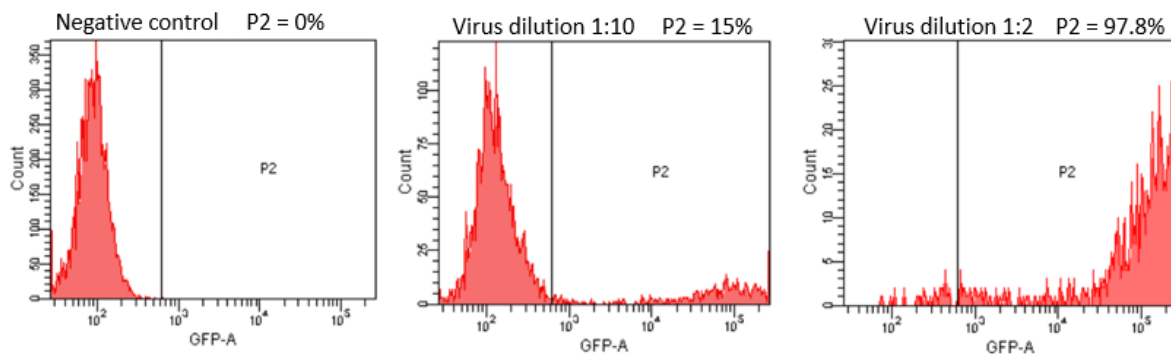


**Figure 4.6. Histograms of JJN3 transduced with eGFP expressing vectors at two different virus dilutions (1:10 and 1:2).** Cells in the P2 region of the histogram were considered as eGFP positive. JJN3 wild type was used as the negative control.

### 4.3.2 Successful overexpression of the glycosyltransferases ST6Gal or B4GalT1 in JJN3 at gene and protein level

qPCR and western blot were used to analyze the gene and protein expression of the two glycosyltransferases ST6Gal1 and B4GalT1 in JJN3 ST6Gal1 or B4GalT1 OE cells. The virus containing supernatant used for transduction was diluted 1:2 or 1:10 before being added to the JJN3 cells. The qPCR results of the ST6Gal1 OE cells (Figure 4.7. A) indicate a gene expression of *ST6GAL1* (virus diluted 1:2), that is 45 times greater than *ST6GAL1* expression in JJN3 wild type. Similar results are seen at protein level with a 34-fold increase in protein expression at virus dilution 1:2 (Figure 4.7 C). JJN3 wild type has little to no expression of either of the transferases as seen both on PCR and western blots. The qPCR result of B4GalT1 OE cells (Figure 4.7 B) shows a solid increase in gene expression of *B4GALT1* compared to JJN3 wild type cells. Corresponding results are seen at protein level (Figure 4.7 D). The overexpression of ST6Gal1 and B4GalT1 is most prominent for the cells transduced with the highest concentration of lentiviruses (dilution 1:2). Therefore, these cells were chosen for further analysis.
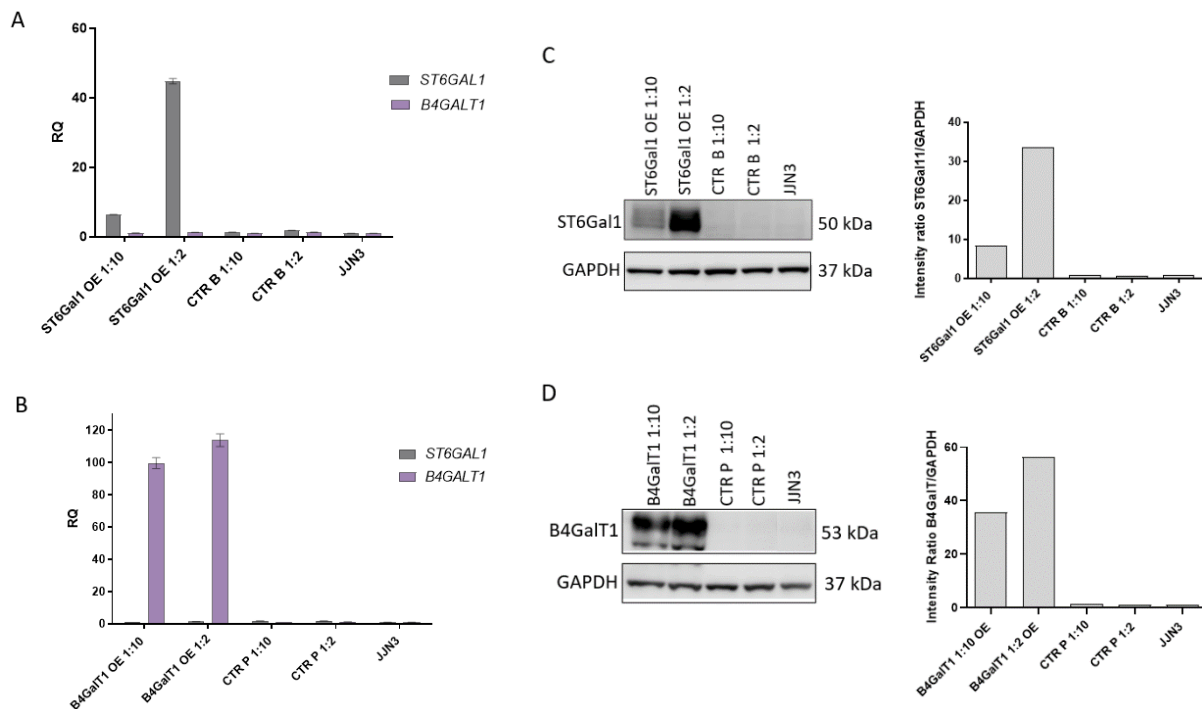


**Figure 4.7. Gene and protein expression of the glycosyltransferases ST6Gal1 and B4GalT1 in JJN3 ST6Gal1/B4GalT1 OE**. A and B: qPCR of JJN3 ST6GAL1 and B4GALT1 OE. JJN3 wild type is used as "reference sample" and beta-actin is the endogenous control. RQ is calculated using the comparative CT method. Bars represent mean ± SD and is calculated from two technical replicates. C: Western blot of JJN3, ST6Gal1 OE and controls (CTR B) showing the protein expression of ST6Gal1. CTR B was transduced with Ex-neg Lv197 Empty and cultured in blasticidin selection medium D: Western blot of JJN3, B4GalT1 and controls (CTR P)

49

showing the protein expression of B4GalT1. CTR P was transduced with Ex-neg-LV105 Empty and cultured in puromycin selection medium. C and D: *GAPDH* was used as loading control when quantitating the protein expression. The protein expression is relative to the protein expression in JJN3 wild type.

### 4.3.3 No alterations in cell viability and doubling time in ST6Gal1- or B4GalT1 overexpressing JJN3 cells.

To investigate if ST6Gal1/B4GalT1 OE cells divide at the same rate as JJN3 wild type, the doubling time was calculated based on four different cell counts, at different times (Figure 4.8 A). The cells were split to a concentration of 0.02/0.04 million cells per ml and cultured for 72 hours before counting. There is no significant difference in the doubling time (around 20 hours) between the ST6Gal1/B4GalT1 OE cells and JJN3/controls.

Flow cytometry (Annexin V-FITC/PI staining) was used to investigate if the overexpression of ST6Gal1 or B4GalT1 in JJN3 influence cell viability (Figure 4.8 B). The scatter plots of the untreated JJN3, control cells (CTR P and CTR B), and S6Gal1 OE and B4GalT1 OE cells show similar percentages (95-96%) of live cells (Q3). Cell viability and cell division appears to be unaffected by the over expression of ST6Gal1 and B4GalT1 in JJN3.

A
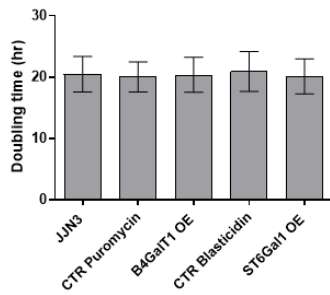


B
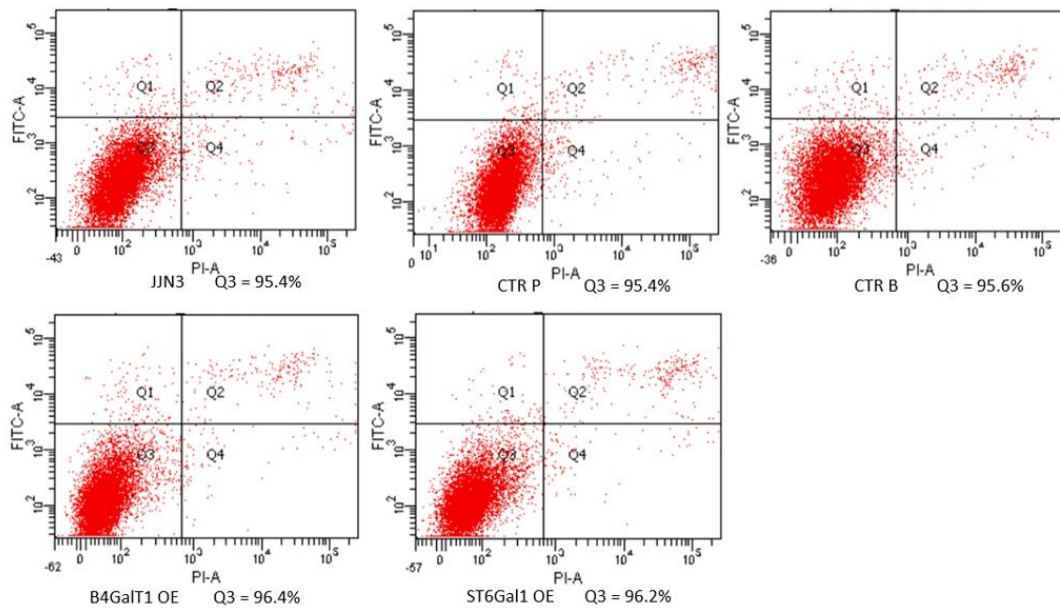


**Figure 4.8. Testing cell growth (doubling time) and cell viability in in JJN3 ST6Gal1OE and B4GalT1 OE cells**. A: The doubling time is calculated as described in the method (2.1.4). The graph is based on four individual cell counts at different times (n=4). Bars represent mean ± SD. B: Cell viability in JJN3 ST6Gal1OE and B4GalT1 OE cells is measured by flow cytometry (Annexin V-FITC/PI staining). Live cells are found in Q3 of the scatter plot. CTR P = Control puromycin (the B4GalT1 OE control), CTR B = Control blasticidin (the ST6GalT1 control).

### 4.3.4 Non conclusive results regarding galactosylation and sialyslation of proteins in ST6Gal1- or B4GalT1 overexpressing JJN3 cells.

Lectin blots were used to investigate if the large increase in the protein expression of ST6Gal1 and B4GalT1 leads to an increase sialylation/galactosylation of proteins. The lectin blot from cell lysate, incubated with the lectin SNA, which binds to sialic acid (Figure 4.9 A) show no apparent differences between ST6Gal1OE or B4GalT1OE and JJN3 wild type/control cells. The lectin blot from cell lysate, incubated with the lectin ECA, which binds to galactose

(Figure 4.9 B) show no sign of an increased amount of galactosylated proteins in B4GalT1 OE compared to JJN3 wild type or control cells.

We also tried to purify IgA from the JJN3 cell lysate, but no successful method was found. A recent study with JJN3 injected into mice showed no M-spike on serum electrophoresis, but kappa light chain was detected by ELISA (data not published). This led us to hypothesize that IgA is not secreted from JJN3 cells. Regardless of this knowledge, there was made an effort to harvest the supernatant from JJN3 to detect the glycosylation of potential IgAs. The blot incubated with SNA (Figure 4.9 C) indicate an increased sialylation in ST6Gal1 OE and B4GalT1 OE compared to their respective controls. However, this increase was not confirmed when repeating the experiment. The bands detected in the lectin blot lay in the area where IgA would be located. However, no bands were detected when incubating the blot with an anti-human IgA antibody IGAH1 (not shown). The blot was also incubated with lectin LCA, to detect N-linked (core structure) glycosylation. No bands were detected in this lectin blot either (data not shown).
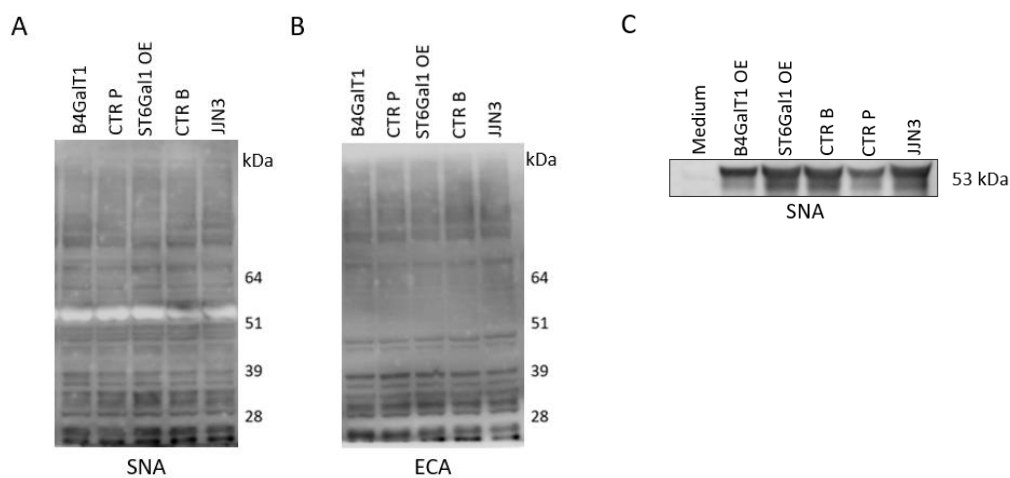


**Figure 4.9. Lectin blot analysis of JJN3 ST6Gal1/B4GalT1 OE cells to detect glycosylation of proteins.** A and B: Total cell lysate from JJN3 wild type, control cells (CTR P and CTR B) and ST6Gal1 OE and B4GalT1 OE cells incubated with A. SNA to detect sialylated proteins and B. ECA to detect galactosylated proteins. C: Lectin blot (SNA) of the supernatant of untreated JJN3 and control cells (CTR P and CTR B) and ST6Gal1 OE and B4GalT1 OE cells. An equal number of cells (400 000 per ml) were seeded out in medium without FBS and with 0.1% BSA. The supernatant was harvested after 24 hours. The figure shows one of two biological replicates. CTR P = control puromycin (the B4GalT1 OE control), CTR B = control blasticidin (the ST6GalT1 control), (FBS= Fetal bovine serum).

## 4.4 Terminal sialic acid residues inhibit the binding of lectin ECA to galactose

As both the manufacturer and our own analysis indicated that terminal sialic acid residues might inhibit lectin ECA from binding to galactose, we performed a lectin blot with M315 protein treated with neuraminidase (Figure 4.10). The enzyme cleaves sialic acid residues from the glycan. The lectin blots show clear binding of ECA in the sample treated with enzyme and no binding of ECA in the untreated sample. The membrane incubated with SNA also show that all sialic acid residues are removed in the sample treated with enzyme.
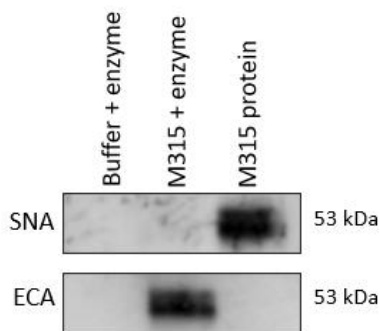


**Figure 4.10. Lectin blots of M315 protein treated with or without neuraminidase (40 U for 24 hours**). One membrane was incubated with SNA, detecting sialic acid, and one membrane was incubated with ECA, detecting galactose. Figure 4.10 show one of three representative experiments.

## 4.5 Decreased IgG Fc sialylation in Vk*myc 12653

Our research group was interested in studying the glycosylation of IgGs from the MM mouse model Vk*myc 12653. These cells induce bone disease in mice (98). Therefore, serum from a mouse injected with Vk*myc 12653 mouse myeloma cells, and an untreated control mouse was collected, and IgG was purified by utilizing Protein G HP SpinTrap. Serum and purified IgG was analyzed by western/lectin blot. One blot was stained with Ponceaus S (Figure 4.11 A), which binds to positive charged amino groups and non-polar regions of proteins. This blot gives an indication of the amount of protein in the different samples. Another blot was incubated with an antibody against IgG (Figure 4.11 B). As expected, there are far more IgGs in the serum obtained from the mouse with MM than the healthy control mouse. The blot incubated with SNA (Figure 4.11 C) reveal that IgGs from the Vk*myc mouse almost completely lack sialic acid. The membrane incubated with ECA (Figure 4.11 D) show more binding of ECA to Vk*myc IgG than the control IgG, but this is most likely because terminal sialic acid residues on CTR IgG inhibit lectin ECA from binding.
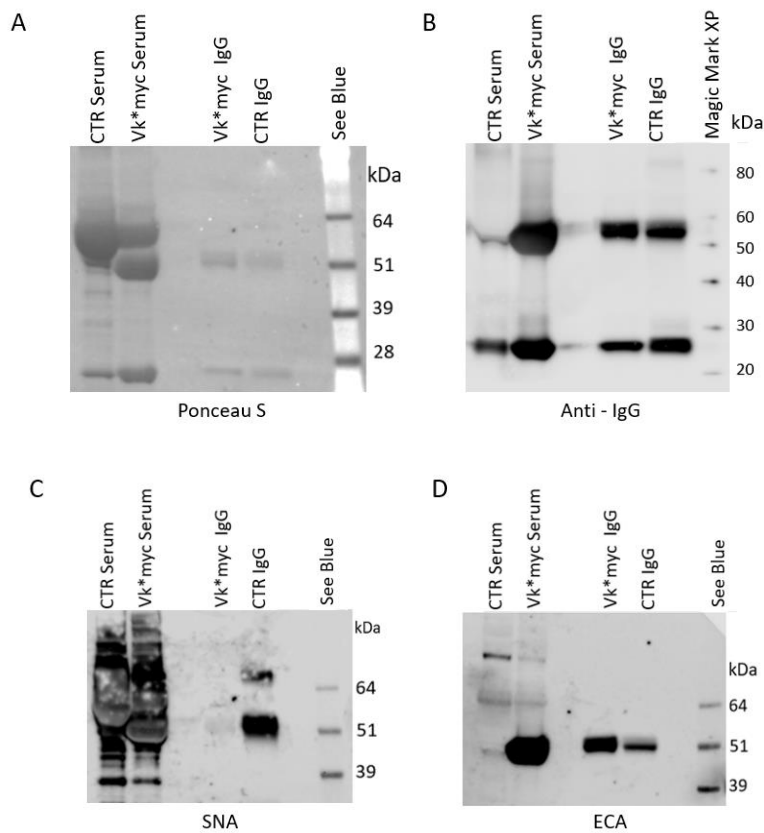
**Figure 4.11. Lectin blots detecting the IgG Fc glycosylation in serum from a Vk*myc 12653-treated mouse.** Serum from a healthy CTR mouse (CTR serum) and a mouse injected with Vk*myc-cells (Vk*myc Serum) and purified IgG from these serum samples is analyzed by western/lectin blot. The figure is made from four identical blots, detecting different monosaccharides/proteins. Serum samples are diluted 1:50, and an equal concentration of purified IgG samples is loaded onto the gel. The figure shows one of two technical replicates. A: Membrane stained with Ponceau S. B: Membrane incubated with an antibody against IgG4. C: Membrane incubated with SNA, D: Membrane incubated with ECA. See Blue and Magic Mark XP are used as mw-standards.

# 5. Discussion

The goal of this project was to establish MM cell lines with modified glycosyltransferase that further could be used to study the effect of Ig glycosylation in MM bone disease. Firstly, the expression of *St6gal1/B4galt1* in MOPC315.BM was knocked down through lentiviral transduction utilizing shRNA. Next, *ST6GAL1*/St6gal1 and *B4GALT1/B4galt1* was overexpressed in the cell lines JJN3 and MOPC315.BM by lentiviral transduction utilizing ORF expression plasmids. Gene and protein expression of the glycosyltransferases were analyzed and the cell viability and doubling time in the modified cells were investigated. Finally, protein glycosylation and glycosylation of Igs from a Vk*myc mouse myeloma model were analyzed.

## 5.1 Modification of ST6Gal1 and B4GalT in MOPC315.BM and JJN3

We hypothesized that altering the expression of the two glycosyltransferases ST6Gal1 and B4GalT1 would lead to changed sialylation and galactosylation of proteins in the cell lines MOPC315.BM and JJN3. The PCR results and western blot analysis from ST6Gal1/B4GalT1 KD in MOPC315.BM and ST6Gal1/B4GalT1 OE in JJN3 indicate a satisfying knockdown/overexpression of ST6Gal1/B4GalT1 at both gene and protein level. As the gene expression of *ST6GALl/St6gal1* and *B4GALT1/B4galt1* is consistent with protein expression, an influence of post transcriptional regulatory mechanisms (e.g., miRNA) seems unlikely. The Lectin blot analysis however did not show any apparent changes in glycosylation status in either intracellular proteins (total cell lysate) or secreted proteins (cell supernatant). It remains to be determined if the sialylation and galactosylation of proteins in the modified cell lines truly is unchanged, or if the method for detection of glycosylation (lectin blots) is inaccurate.

As described in section 1.5.2.2 is ST6Gal1 the glycosyltransferase responsible for adding terminal sialic acid to N-glycans in a α2-6 linkage to galactose. Terminal sialic acid residues in N-glycans can also be linked to galactose in a α2-3 linkage (catalyzed by ST3Gal), but this linkage is not observed in N-glycans of Igs (60), (30). B4GalT1 is the glycosyltransferase responsible for adding terminal galactose to N-glycans in a β1-4 linkage to GlcNAc. One study found a 90% reduction in galactosylated serum proteins in B4GalT1 knockout mice. (58). These findings demonstrate the essential role of B4GalT1 in N-linked glycosylation of serum proteins. Other researchers have successfully modified the expression of ST6Gal1 and B4GalT1 in other cell lines/mice and observed altered protein sialylation and galactosylation

(57), (58), (99). No compensatory changes were found when modifying various glycosyltransferases (including ST6Gal1 and B4GalT1) in Chinese hamster ovary cells (100). Our lectin blot analyzes from total cell lysate show no apparent decrease in sialylation and galactosylation of proteins in MOPC315.BM ST6Gal1/B4GalT1 KD. There is not reported compensatory changes in the form of increased expression of other enzymes of the B4GalT/ST6Gal family, but it is a theoretical possibility that such chances could occur. Analyses of the gene/protein expression of other glycosyltransferases would reveal whether this was the case. It should be emphasized that B4GalT1 is the main, but not the only enzyme responsible for galactosylation of N-glycans. It is also clear from the western blot analysis that there is still a significant protein expression of B4GalT1 some of the B4GalT1 KD clones. Regarding the OE of ST6Gal1/B4GalT1 in JJN3, the lectin blots from total cell lysate show no apparent increase in protein sialylation/galactosylation despite a clear increase in gene and protein expression of ST6Gal1/B4GalT1. It is striking how the lectin blot from total cell lysate from JJN3 show heavily sialylated/galactosylated proteins, even though ST6Gal1 and B4GalT1 is barely expressed in JJN3 wild type. These results indicate that the lectin blot analysis might not be specific enough to capture the exact changes caused by modification of ST6Gal1/B4GalT1. The lack of increased sialylation despite increased protein expression of ST6Gal1 might be explained by the fact that ST6Gal1 is dependent on the presence of terminal galactose residues to add sialic acid to the structure. As *ST6GAL1* and *B4GALT1* ORF plasmids was not co-transduced, there could be a lack of terminal galactose residues on N-glycans, making sialylation impossible.

We know from previous research that *ST6GAL1* and *B4GALT1* is downregulated in MM patients with bone disease compared to patients without bone disease (41). In the same study, it was also shown that sialylation and galactosylation of the Igs was reduced. However, this does not necessarily mean that there is a direct correlation between the two. Also, it is important to keep in mind that there might be differences between MM cell lines and primary cells when it comes to glycosylation. Moreover, we have not taken into consideration potential removal of sialic acid (catalyzed by neuraminidases) or galactose (catalyzed by β-galactosidase) or limiting amounts of nucleotide sugars (donor sugars) in the cell culture. The biosynthesis of glycoproteins is a complex process and when culturing a cell line, factors like nutrient levels, dissolved oxygen, pH, temperature, and by-product accumulation can affect

protein glycosylation. As these factors will affect the glycosylation pathway, they should be monitored closely when culturing a cell line *in vitro* (101).

### 5.1.1. Lectin specificity

The conflicting results between protein expression of the glycosyltransferases and extent of glycosylation might be due to weakness in the lectin blot method. A study found that ECL lectin might also recognize galactose bound to GalNAc in a β1-3 linkage (65). The formation of this linkage is mediated by core 1 beta-1,3-galactosyltransferase (C1B3GalT) and is found in core 1 O-glycans (33). The hinge region of IgA1 is heavily O-glycosylated and might be detected by lectin ECA. Lectin blot analysis of M315 protein treated with neuraminidase (Figure 4.10) revealed that terminal sialic acid residues completely block lectin ECL from binding. This is important to take into consideration when interpreting the results from blots incubated with ECA, as this means that all galactosylated proteins in the cell detected by ECA are not sialylated. Lectin SNA binds to sialic acid bound to both galactose and GalNAc in a α2-6 linkage. It also binds to some degree sialic acid bound to galactose in a α2-3 linkage (95), (65). Sialic acid in N-glycans is bound to galactose in a α2-6 or α2-3 linkage. Sialic acid in O-glycans, for instance in IgA1 are bound to GalNAc in a α2-6 linkage or to galactose in a α2-3 linkage (33). Because lectin SNA binds to sialic acid in different linkages (both galactose and GalNAc) it will not only detect sialic acid in Ig N-glycans bound to galactose in α2-6 linkage. This makes it challenging to interpret results from the lectin blot analyses.

### 5.1.2. Glycosylation of IgA in MOC315.BM and JJN3

The glycosylation status of secreted proteins from MOPC315.BM ST6Gal1/B4GalT1 KD clones was analyzed by lectin blots (Figure 4.4 C). The blots were incubated with ECA, SNA and LCA. In the blot incubated with ECA there were no bands detected. This is probably due to sialic acid residues blocking the lectin from binding. The blots incubated with LCA, detecting core N-glycosylation, showed relatively weak bands compared to the blot incubated with SNA. This might be due to weak binding of the lectin itself, or it might be because it is not a lot of N-linked glycosylation present. The bands detected when incubating with SNA is weaker in ST6Gal1 KD and B4GalT1 KD compared to the control clone, however this difference is not statistically significant, and the standard deviation is relatively large.

When analyzing the supernatant of JJN3 ST6Gal1/B4GalT1 OE (Figure 4.9 C), no bands were detected when incubating with ECA or LCA. There were also no bands detected when incubating with an antibody against IGAH1. The band detected when incubating the blot with SNA lectin lay in the area where IgA heavy chain would be located. It is not possible to say with certainty that this is sialylation of IgA heavy chain, but it is likely. The antibody used to detect IgA heavy chain might not bind because of the low protein concentration of the supernatant. There are barely any protein present in the supernatant, and we were not able to determine the protein concentration by utilizing Bradford protein assay (linear range 125-1000 µg/ml). Since no bands were detected when incubating the blot with LCA, it is reasonable to assume that the sialylation detected is not N-linked glycosylation and might therefor be O-linked glycosylation. Sialylation appears to be increased in ST6Gal1 OE and B4GalT1 OE compared to their respective controls. However, these results were not confirmed when repeating the experiment.

We experienced large differences and conflicting results between experiments when performing lectin blots of the supernatant from both MOPC315 and JJN3. Lectin blot analysis from the supernatant of MOPC315.BM KD was performed three times and we observed a substantial standard deviation. We also experienced this when performing technical replicates. The varying results might be due to the low protein concentration in the supernatant, making small variations in the technical performance have a large impact on the results. Since the protein concentration of the supernatant was so low it was not detectable using Bradford protein assay, it was not possible to ensure that an equal amount of protein was loaded onto the gel. The protein in the supernatant was also not detected when staining with Ponceau S. The only measure we could take to equalize the protein concentration, was to seed out an equal number of cells 24 hours prior to harvesting the supernatant. This is evidently not an optimal tactic, as the amount of Igs secreted by the modified cells might differ.

Unfortunately, we were not able to analyze the galactosylation of proteins in the supernatant due to potential galactose residues being blocked by terminal sialic acid residues. A natural next step would be to try to remove sialic acid residues by utilizing neuraminidase, and thereby be able to observe potential protein galactosylation. This was not done due to the low protein concentration of the supernatant. It might however be possible to concentrate the supernatant and thereafter treat the samples with neuraminidase. The most ideal solution

would be to purify IgA from either the supernatant or cell lysate to ensure optimal buffer conditions for enzyme activity.

### 5.1.3. Alternative methods to examine glycosylation of proteins

We also tried to analyze membrane protein glycosylation (results not included in this thesis) by lectin flow. Surface membrane glycosylation can be analyzed by flow cytometry utilizing biotinylated lectins and fluorochrome conjugated streptavidin. In the pilot analysis, streptavidin conjugated with APC-Cy7 was used to visualize the binding of the lectins (SNA, ECA and LCA). This experiment showed more promising results in terms of decreased or increased sialylation and galactosylation of proteins in KD and OE cells. Why we were able to observe changes in surface protein glycosylation and not in intracellular proteins is unclear. Lectin flow might be a useful method to analyze general surface protein glycosylation but will not provide information about Ig glycosylation specifically. Since the lectin blot/flow analysis might not be the optimal method to analyze the glycosylation of IgA, other methods like matrix assisted laser desorption/ionization (MALDI)-time of flight (TOF)-mass spectrometry (MS), high performance liquid chromatography (HPLC) MS might be more suitable. It would be useful to analyze the glycosylation of IgA from the wild type cell lines (JJN3 and MOPC315). The protein expression of ST6Gal1 and B4GalT1 was analyzed prior to KD and OE, but we did not perform an analysis of the glycosylation of IgA in the selected cell lines. Given that the degree of sialylation and galactosylation of IgA correlates with the protein expression of ST6Gal1 and B4GalT1, we would expect so see little to no sialylation and galactosylation of IgAs from JJN3 wild type. For MOPC315.BM, which has an adequate protein expression of ST6Gal1 and B4GalT1, we would expect a greater amount of IgAs to be sialylated and galactosylated. Additionally, it would be helpful to analyze the sialylation and galactosylation of ST6Gal1/B4GalT1 OE/KD cells utilizing mass spectrometry. Such an analysis would give a more accurate picture of the glycosylation status of IgA in the modified cell lines, making it possible to draw a conclusion of whether it is possible to modify the glycosylation in these specific cell lines by knocking down/overexpressing glycosyltransferases.

### 5.1.4 Unsuccessful attempt to overexpression of ST6Gal1 and B4GalT1 in MOPC315.BM

The attempt to overexpress *St6Gal1/B4galt1* in MOPC315.BM was not successful. The flow cytometry analysis of the eGFP positive control revealed a low amount of the eGFP positive

MOPC315.BM cells, indicating a low infection percentage. PCR results did not indicate any overexpression of *St6gal1/B4galt1*. We also experienced slow cell growth after transduction. This is likely due to the low transduction percentage, leading to a high percentage of cells not being puromycin resistant. To ensure that the optimal multiplicity of infection (MOI) was used in the transduction, it is possible to use the eGFP positive control to perform a virus titer utilizing a range of different MOIs. Since we observed a relatively low expression of eGFP when diluting the virus 1:2, it is however not likely that doubling the concentration would give a satisfying percentage of eGFP positive cells. A more optimal option would be to co-transduce the gene of interest with a marker (e.g., eGFP), making it possible to sort out the transduced cells by fluorescence-activated cell sorting (FACS).

## 5.2 Unchanged cell growth and viability in cell lines with modified glycosyltransferases

The purpose of creating MM cell lines with modified glycosyltransferases was to use these cell lines in future *in vivo* studies (in mice). When modifying a cell line, it is necessary to examine if the growth rate and cell viability is altered. If modifications done to the cell line influence viability and growth rate, this will influence the aggressivity and rate of cancer development in the research animal. It is therefore desirable to be aware of how the modified cell line grow *in vitro* before injecting the cells into laboratory animals. The results presented in this thesis indicate that modification of ST6Gal1/B4GalT1 in MOPC315.BM and JJN3 do not influence the doubling time or the viability of the cells. The flow cytometry analysis (Annexin V-FITC/PI staining) was only performed once and should be repeated to confirm the results. Observing cells in microscope did not indicate any difference in cell viability between modified cells and wild type cells. We tried to analyze the metabolic activity (ATP production) to confirm equal cell viability among modified cell lines. Due to the assay sensitivity for variations in cell number we found this assay not to be optimal for testing viability in the modified cells.

## 5.3 Decreased sialylation of IgG from Vk*myc 12653 mouse

Lectin blot analysis (Figure 4.11) revealed a decreased sialylation of IgG from the mouse injected with Vk*myc myeloma cells. Murine IgG has one conserved seat for N-linked glycosylation in the Fc region of each heavy chain (38). It is well established that the glycosylation status of the Fc region plays a central role in regulating the effector functions of

the Ig. Current research conclude that the Ig sialylation have an anti-inflammatory effect and that loss of sialic acid is associated with autoimmune diseases like RA, inflammatory bowel disease, IgAN and SLE (102), (30), (103). Research also suggested that bone loss in RA is partly due to desialylated Igs forming Ig-complexes, which stimulates osteoclast differentiation (45). Our research group has found that Ig sialylation was reduced in a myeloma mouse model (injected with 5TGM1 myeloma cell line) upon disease progression, and when treating these mice with ManNac, the mice showed a reduced number of bone lesions and reduced tumor load compared to control mice treated with mannose (41).

The results from the lectin blot analysis indicate that the Vk*myc may well be a useful myeloma mouse model to further study the effects of ManNAc treatment. When injecting Vk*myc myeloma cells into mice, the mice develop MM with the associated bone disease and a high secretion of monoclonal IgGs (subtype IgG2b) (97). Vk*myc cells are dependent on the microenvironment of the BM and have not been successfully cultured *in vitro* but are maintained by transplantation into mice. Thus, the environmental factors that might influence the biosynthesis of glycoproteins are more comparable to those of a MM patient, than for example a MM cell line cultured *in vitro*. Utilizing primary cells that do not grow *in vitro* to investigate Ig glycosylation has some limitations, as this means that the cells cannot be genetically altered or explored in the lab. There is now an ongoing *in vivo* study where Vk*myc (12653) cells are injected into mice, followed by treatment with either ManNAc or mannose. Analysis of the glycosylation of Igs from mice treated with ManNAc and mannose will be analyzed by mass spectrometry and will give further insight in whether ManNAc is a possible treatment option for MM bone disease.

# 6. Conclusion

In this project the gene end protein expression of the two glycosyltransferases ST6Gal1 and B4GalT1 was successfully overexpressed in the cell lines JJN3 and MOPC315.BM and knocked down in the cell line MOPC315.BM. Analysis of whether the knockdown and overexpression of these transferases cause a decreased/increased sialylation/galactosylation of immunoglobulins gave non-conclusive results. Both the method utilized (lectin blotting) and limiting factors, like not being able to purify IgA from the cell lines, makes it impossible to draw a definite conclusion. It may well be that glycosylation of Igs in these cell lines is controlled and influenced by other factors both intracellularly and extracellularly (culture conditions), and therefor do not show a correlation between protein expression of the glycosyltransferases and glycosylation of proteins. Another method, like mass spectrometry, could be utilized to give a more conclusive result regarding sialylation and galactosylation of Igs in the modified cell lines. According to the results presented in this thesis, cell doubling time and viability is unchanged when modifying the expression of ST6Gal1and B4GalT1 in the cell lines MOPC315.BM and JJN3. Lectin blot analysis of a Vk*myc myeloma mouse model revealed a clear decrease in sialylation of serum IgGs compared to the healthy control. As decreased sialylation of Igs is thought to be a driver of osteoclastogenesis, ManNAc is being studied as a potential treatment option for bone loss. Because the Vk*myc myeloma mouse model, according to the findings in this project, lack terminal sialic acid residues in Ig glycans, this mouse model might be a suitable model to further investigate the effects of ManNAc treatment. However, an evident limitation of utilizing these cells is that, as of today, they cannot be cultured *in vitro*.

# References

1.	Bianchi G, Munshi NC. Pathogenesis beyond the cancer clone(s) in multiple myeloma. Blood. 2015;125(20):3049-58.
2.	Pawlyn C, Morgan GJ. Evolutionary biology of high-risk multiple myeloma. Nat Rev Cancer. 2017;17(9):543-56.
3.	Kyle RA, Gertz MA, Witzig TE, Lust JA, Lacy MQ, Dispenzieri A, et al. Review of 1027 Patients With Newly Diagnosed Multiple Myeloma. Mayo Clinic Proceedings. 2003;78(1):21-33.
4.	Rajkumar SV, Dimopoulos MA, Palumbo A, Blade J, Merlini G, Mateos MV, et al. International Myeloma Working Group updated criteria for the diagnosis of multiple myeloma. Lancet Oncol. 2014;15(12):e538-48.
5.	Kreftregisteret. 2019 [Available from: https://sb.kreftregisteret.no/insidens/.
6.	Palumbo A, Anderson K. Multiple myeloma. N Engl J Med. 2011;364(11):1046-60.
7.	Kyle RA, Rajkumar SV. Criteria for diagnosis, staging, risk stratification and response assessment of multiple myeloma. Leukemia. 2009;23(1):3-9.
8.	Kyle RA, Durie BGM, Rajkumar SV, Landgren O, Blade J, Merlini G, et al. Monoclonal gammopathy of undetermined significance (MGUS) and smoldering (asymptomatic) multiple myeloma: IMWG consensus perspectives risk factors for progression and guidelines for monitoring and management. Leukemia. 2010;24(6):1121-7.
9.	Kyle RA, Therneau TM, Rajkumar SV, Larson DR, Plevak MF, Offord JR, et al. Prevalence of monoclonal gammopathy of undetermined significance. N Engl J Med. 2006;354(13):1362-9.
10.	Barilà G, Bonaldi L, Grassi A, Martines A, Liço A, Macrì N, et al. Identification of the true hyperdiploid multiple myeloma subset by combining conventional karyotyping and FISH analysis. Blood Cancer Journal. 2020;10(2):18.
11.	Manier S, Salem KZ, Park J, Landau DA, Getz G, Ghobrial IM. Genomic complexity of multiple myeloma and its clinical implications. Nat Rev Clin Oncol. 2017;14(2):100-13.
12.	Morgan GJ, Walker BA, Davies FE. The genetic architecture of multiple myeloma. Nat Rev Cancer. 2012;12(5):335-48.
13.	Fonseca R, Abouzaid S, Bonafede M, Cai Q, Parikh K, Cosler L, et al. Trends in overall survival and costs of multiple myeloma, 2000–2014. Leukemia. 2017;31(9):1915-21.
14.	Langseth Ø O, Myklebust T, Johannesen TB, Hjertner Ø, Waage A. Incidence and survival of multiple myeloma: a population-based study of 10 524 patients diagnosed 1982-2017. Br J Haematol. 2020;191(3):418-25.
15.	Pinto V, Bergantim R, Caires HR, Seca H, Guimarães JE, Vasconcelos MH. Multiple Myeloma: Available Therapies and Causes of Drug Resistance. Cancers (Basel). 2020;12(2):407.
16.	Roodman GD. Pathogenesis of myeloma bone disease. Leukemia. 2009;23(3):435-41.
17.	Terpos E, Morgan G, Dimopoulos MA, Drake MT, Lentzsch S, Raje N, et al. International Myeloma Working Group recommendations for the treatment of multiple myeloma-related bone disease. J Clin Oncol. 2013;31(18):2347-57.
18.	Terpos E, Ntanasis-Stathopoulos I, Gavriatopoulou M, Dimopoulos MA. Pathogenesis of bone disease in multiple myeloma: from bench to bedside. Blood cancer journal. 2018;8(1):7-.
19.	Bonewald LF. The amazing osteocyte. Journal of Bone and Mineral Research. 2011;26(2):229-38.
20.	Hadjidakis DJ, Androulakis, II. Bone remodeling. Ann N Y Acad Sci. 2006;1092:385-96.
21.	Gaur T, Lengner CJ, Hovhannisyan H, Bhat RA, Bodine PVN, Komm BS, et al. Canonical WNT Signaling Promotes Osteogenesis by Directly Stimulating Runx2 Gene Expression*. Journal of Biological Chemistry. 2005;280(39):33132-40.
22.	Lin GL, Hankenson KD. Integration of BMP, Wnt, and notch signaling pathways in osteoblast differentiation. J Cell Biochem. 2011;112(12):3491-501.

23.     Shinohara M, Takayanagi H. Novel osteoclast signaling mechanisms. Current Osteoporosis Reports. 2007;5(2):67-72.

24.     Kim JH, Kim N. Signaling Pathways in Osteoclast Differentiation. Chonnam Med J. 2016;52(1):12-7.

25.     Koga T, Inui M, Inoue K, Kim S, Suematsu A, Kobayashi E, et al. Costimulatory signals mediated by the ITAM motif cooperate with RANKL for bone homeostasis. Nature. 2004;428(6984):758-63.

26.     Pearse RN, Sordillo EM, Yaccoby S, Wong BR, Liau DF, Colman N, et al. Multiple myeloma disrupts the TRANCE/ osteoprotegerin cytokine axis to trigger bone destruction and promote tumor progression. Proc Natl Acad Sci U S A. 2001;98(20):11581-6.

27.     Brunetti G, Oranger A, Mori G, Specchia G, Rinaldi E, Curci P, et al. Sclerostin is overexpressed by plasma cells from multiple myeloma patients. Ann N Y Acad Sci. 2011;1237:19-23.

28.     Terpos E, Christoulas D, Gavriatopoulou M. Biology and treatment of myeloma related bone disease. Metabolism. 2018;80:80-90.

29.     Henry DH, Costa L, Goldwasser F, Hirsh V, Hungria V, Prausova J, et al. Randomized, double-blind study of denosumab versus zoledronic acid in the treatment of bone metastases in patients with advanced cancer (excluding breast and prostate cancer) or multiple myeloma. J Clin Oncol. 2011;29(9):1125-32.

30.     Reily C, Stewart TJ, Renfrow MB, Novak J. Glycosylation in health and disease. Nature Reviews Nephrology. 2019;15(6):346-66.

31.     Boune S, Hu P, Epstein AL, Khawli LA. Principles of N-Linked Glycosylation Variations of IgG-Based Therapeutics: Pharmacokinetic and Functional Considerations. Antibodies (Basel). 2020;9(2):22.

32.     Zhang Z, Westhrin M, Bondt A, Wuhrer M, Standal T, Holst S. Serum protein N-glycosylation changes in multiple myeloma. Biochimica et Biophysica Acta (BBA) - General Subjects. 2019;1863(5):960-70.

33.     Ohyama Y, Yamaguchi H, Nakajima K, Mizuno T, Fukamachi Y, Yokoi Y, et al. Analysis of O-glycoforms of the IgA1 hinge region by sequential deglycosylation. Scientific Reports. 2020;10(1):671.

34.     Novak J, Julian BA, Tomana M, Mestecky J. IgA glycosylation and IgA immune complexes in the pathogenesis of IgA nephropathy. Semin Nephrol. 2008;28(1):78-87.

35.     Dall'Olio F, Vanhooren V, Chen CC, Slagboom PE, Wuhrer M, Franceschi C. N-glycomic biomarkers of biological aging and longevity: A link with inflammaging. Ageing Research Reviews. 2013;12(2):685-98.

36.     Steffen U, Koeleman CA, Sokolova MV, Bang H, Kleyer A, Rech J, et al. IgA subclasses have different effector functions associated with distinct glycosylation profiles. Nature Communications. 2020;11(1):120.

37.     Kim H, Yamaguchi Y, Masuda K, Matsunaga C, Yamamoto K, Irimura T, et al. O-glycosylation in hinge region of mouse immunoglobulin G2b. Journal of Biological Chemistry. 1994;269(16):12345-50.

38.     Zaytseva OO, Jansen BC, Hanić M, Mrčela M, Razdorov G, Stojković R, et al. MIgGGly (mouse IgG glycosylation analysis) - a high-throughput method for studying Fc-linked IgG N-glycosylation in mice with nanoUPLC-ESI-MS. Scientific Reports. 2018;8(1):13688.

39.     de Haan N, Reiding KR, Krištić J, Hipgrave Ederveen AL, Lauc G, Wuhrer M. The N-Glycosylation of Mouse Immunoglobulin G (IgG)-Fragment Crystallizable Differs Between IgG Subclasses and Strains. Frontiers in immunology. 2017;8:608-.

40.     Phillips-Quagliata JM. Mouse IgA allotypes have major differences in their hinge regions. Immunogenetics. 2002;53(12):1033-8.

41.     Westhrin M, Kovcic V, Zhang Z, Moen SH, Nedal TMV, Bondt A, et al. Monoclonal immunoglobulins promote bone loss in multiple myeloma. Blood. 2020;136(23):2656-66.

42.     Engdahl C, Bang H, Dietel K, Lang SC, Harre U, Schett G. Periarticular Bone Loss in Arthritis Is Induced by Autoantibodies Against Citrullinated Vimentin. Journal of Bone and Mineral Research. 2017;32(8):1681-91.

43.     Dusad A, Duryee MJ, Shaw AT, Klassen LW, Anderson DR, Wang D, et al. Induction of bone loss in DBA/1J mice immunized with citrullinated autologous mouse type II collagen in the absence of adjuvant. Immunol Res. 2014;58(1):51-60.

44.     Harre U, Georgess D, Bang H, Bozec A, Axmann R, Ossipova E, et al. Induction of osteoclastogenesis and bone loss by human autoantibodies against citrullinated vimentin. J Clin Invest. 2012;122(5):1791-802.

45.     Harre U, Lang SC, Pfeifle R, Rombouts Y, Frühbeißer S, Amara K, et al. Glycosylation of immunoglobulin G determines osteoclast differentiation and bone loss. Nature Communications. 2015;6(1):6651.

46.     Anthony RM, Nimmerjahn F. The role of differential IgG glycosylation in the interaction of antibodies with FcγRs in vivo. Current Opinion in Organ Transplantation. 2011;16(1).

47.     Anthony RM, Wermeling F, Ravetch JV. Novel roles for the IgG Fc glycan. Ann N Y Acad Sci. 2012;1253:170-80.

48.     Tomana M, Schrohenloher RE, Reveille JD, Arnett FC, Koopman WJ. Abnormal galactosylation of serum IgG in patients with systemic lupus erythematosus and members of families with high frequency of autoimmune diseases. Rheumatol Int. 1992;12(5):191-4.

49.     Rombouts Y, Ewing E, van de Stadt LA, Selman MH, Trouw LA, Deelder AM, et al. Anti-citrullinated protein antibodies acquire a pro-inflammatory Fc glycosylation phenotype prior to the onset of rheumatoid arthritis. Ann Rheum Dis. 2015;74(1):234-41.

50.     Biermann MH, Griffante G, Podolska MJ, Boeltz S, Stürmer J, Muñoz LE, et al. Sweet but dangerous - the role of immunoglobulin G glycosylation in autoimmunity and inflammation. Lupus. 2016;25(8):934-42.

51.     Shimozato S, Hiki Y, Odani H, Takahashi K, Yamamoto K, Sugiyama S. Serum under-galactosylated IgA1 is increased in Japanese patients with IgA nephropathy. Nephrology Dialysis Transplantation. 2008;23(6):1931-9.

52.     Yan Y, Xu LX, Zhang JJ, Zhang Y, Zhao MH. Self-aggregated deglycosylated IgA1 with or without IgG were associated with the development of IgA nephropathy. Clin Exp Immunol. 2006;144(1):17-24.

53.     Gomes MM, Wall SB, Takahashi K, Novak J, Renfrow MB, Herr AB. Analysis of IgA1 N-glycosylation and its contribution to FcalphaRI binding. Biochemistry. 2008;47(43):11285-99.

54.     Oortwijn BD, Roos A, van der Boog PJM, Klar-Mohamad N, van Remoortere A, Deelder AM, et al. Monomeric and polymeric IgA show a similar association with the myeloid FcαRI/CD89. Molecular Immunology. 2007;44(5):966-73.

55.     Neelamegham S, Mahal LK. Multi-level regulation of cellular glycosylation: from genes to transcript to enzyme to structure. Curr Opin Struct Biol. 2016;40:145-52.

56.     Amado M, Almeida R, Schwientek T, Clausen H. Identification and characterization of large galactosyltransferase gene families: galactosyltransferases for all functions1. Biochimica et Biophysica Acta (BBA) - General Subjects. 1999;1473(1):35-53.

57.     Keusch J, Lydyard PM, Delves PJ. The effect on IgG glycosylation of altering beta1, 4-galactosyltransferase-1 activity in B cells. Glycobiology. 1998;8(12):1215-20.

58.     Kido M, Asano M, Iwakura Y, Ichinose M, Miki K, Furukawa K. Normal levels of serum glycoproteins maintained in beta-1, 4-galactosyltransferase I-knockout mice. FEBS Lett. 1999;464(1-2):75-9.

59.     Lee J, Sundaram S, Shaper NL, Raju TS, Stanley P. Chinese Hamster Ovary (CHO) Cells May Express Six β4-Galactosyltransferases (β4GalTs): CONSEQUENCES OF THE LOSS OF FUNCTIONAL β4GalT-1, β4GalT-6, OR BOTH IN CHO GLYCOSYLATION MUTANTS*. Journal of Biological Chemistry. 2001;276(17):13924-34.

60.     Dall'Olio F. The sialyl-alpha2,6-lactosaminyl-structure: biosynthesis and functional role. Glycoconj J. 2000;17(10):669-76.

61.     Takashima S, Tsuji S. ST6 Beta-Galactoside Alpha-2,6-Sialyltranferase 2 (ST6GAL2). In: Taniguchi N, Honke K, Fukuda M, Narimatsu H, Yamaguchi Y, Angata T, editors. Handbook of Glycosyltransferases and Related Genes. Tokyo: Springer Japan; 2014. p. 705-14.

62.     Laporte B, Gonzalez-Hilarion S, Maftah A, Petit J-M. The second bovine β-galactoside-α2,6-sialyltransferase (ST6Gal II): genomic organization and stimulation of its in vitro expression by IL-6 in bovine mammary epithelial cells. Glycobiology. 2009;19(10):1082-93.

63.     Rohfritsch PF, Joosten JAF, Krzewinski-Recchi M-A, Harduin-Lepers A, Laporte B, Juliant S, et al. Probing the substrate specificity of four different sialyltransferases using synthetic β-d-Galp-(1→4)-β-d-GlcpNAc-(1→2)-α-d-Manp-(1→O) (CH2)7CH3 analogues: General activating effect of replacing N-acetylglucosamine by N-propionylglucosamine. Biochimica et Biophysica Acta (BBA) - General Subjects. 2006;1760(4):685-92.

64.     Lam SK, Ng TB. Lectins: production and practical applications. Applied Microbiology and Biotechnology. 2011;89(1):45-55.

65.     Iskratsch T, Braun A, Paschinger K, Wilson IBH. Specificity analysis of lectins and antibodies using remodeled glycoproteins. Analytical Biochemistry. 2009;386(2):133-46.

66.     Martin LT, Marth JD, Varki A, Varki NM. Genetically Altered Mice with Different Sialyltransferase Deficiencies Show Tissue-specific Alterations in Sialylation and Sialic Acid 9-O-Acetylation*210. Journal of Biological Chemistry. 2002;277(36):32930-8.

67.     Wu AM, Wu JH, Tsai M-S, Yang Z, Sharon N, Herp A. Differential affinities of Erythrina cristagalli lectin (ECL) toward monosaccharides and polyvalent mammalian structural units. Glycoconjugate Journal. 2007;24(9):591-604.

68.     Gooding RP, Bybee A, Cooke F, Little A, Marsh SG, Coelho E, et al. Phenotypic and molecular analysis of six human cell lines derived from patients with plasma cell dyscrasia. Br J Haematol. 1999;106(3):669-81.

69.     Hofgaard PO, Jodal HC, Bommert K, Huard B, Caers J, Carlsen H, et al. A novel mouse model for multiple myeloma (MOPC315.BM) that allows noninvasive spatiotemporal detection of osteolytic disease. PLoS One. 2012;7(12):e51892.

70.     Acosta-Alvear D, Hann BC, Rabinovich BA, Shuman MA, Walter P. Multi-Modality Imaging of Multiple Myeloma Bone Disease In Orthotopic Xenograft Models. Blood. 2010;116(21):5014-.

71.     Moore CB, Guthrie EH, Huang MT-H, Taxman DJ. Short hairpin RNA (shRNA): design, delivery, and assessment of gene knockdown. Methods Mol Biol. 2010;629:141-58.

72.     Martin K. Introduction to Competent Cells  [Available from: https://www.goldbio.com/articles/article/Introduction-to-Competent-Cells#_Toc27037972.

73.     Bergmans HE, van Die IM, Hoekstra WP. Transformation in Escherichia coli: stages in the process. Journal of Bacteriology. 1981;146(2):564.

74.     Sigma-Adrich. Competent Cell Compendium:

Tools and Tips for Successful Transformations  [Available from: https://www.sigmaaldrich.com/content/dam/sigma-aldrich/life-science/cloning-and-expression/compcellscompend.pdf.

75.     Promega. PureYield™ Plasmid Miniprep System 2009 [Available from: https://no.promega.com/-/media/files/resources/protocols/technical-bulletins/101/pureyield-plasmid-miniprep-system-protocol.pdf?la=en.

76.     Qiagen. Key Steps In Plasmid Purification Protocols  [Available from: https://www.qiagen.com/us/knowledge-and-support/knowledge-hub/technology-and-research/plasmid-resource-center/key-steps-in-plasmid-purification-protocols.

77.     Bojar D. HEK293: AN ESSENTIAL HUMAN CELL LINE WITH A UNEXPECTED ORIGIN 2020 [Available from: https://blog.genofab.com/hek293-cell-line.

78.     Gándara C, Affleck V, Stoll EA. Manufacture of Third-Generation Lentivirus for Preclinical Use, with Process Development Considerations for Translation to Good Manufacturing Practice. Hum Gene Ther Methods. 2018;29(1):1-15.

79.     Miyoshi H, Blömer U, Takahashi M, Gage FH, Verma IM. Development of a self-inactivating lentivirus vector. J Virol. 1998;72(10):8150-7.

80.     White JM, Delos SE, Brecher M, Schornberg K. Structures and mechanisms of viral membrane fusion proteins: multiple variations on a common theme. Crit Rev Biochem Mol Biol. 2008;43(3):189-219.

81.     Qiagen. RNeasy Mini Handbook [Available from: https://www.qiagen.com/us/resources/download.aspx?id=14e7cf6e-521a-4cf7-8cbc-bf9f6fa33e24&lang=en.

82.     ThermoFisher. Reverse Transcription Reaction Setup—Seven Important Considerations [

83.     ThermoFisher. Introduction to Gene Expression [Available from: https://www.thermofisher.com/document-connect/document-connect.html?url=https%3A%2F%2Fassets.thermofisher.com%2FTFS-Assets%2FLSG%2Fmanuals%2F4454239_IntrotoGeneEx_GSG.pdf&title=TWFudWFsOiBJbnRyb2R1Y3Rpb24gdG8gR2VuZSBFeHByZXNzaW9uIEdldHRpbmcgU3RhcnRlZCBHdWlkZSAoRW5nbGlzaCAp.

84.     ThermoFisher. PCR Basics [Available from: https://www.thermofisher.com/no/en/home/life-science/cloning/cloning-learning-center/invitrogen-school-of-molecular-biology/pcr-education/pcr-reagents-enzymes/pcr-basics.html.

85.     ThermoFisher. How TaqMan Assays Work [Available from: https://www.thermofisher.com/no/en/home/life-science/pcr/real-time-pcr/real-time-pcr-learning-center/real-time-pcr-basics/how-taqman-assays-work.html.

86.     Mahmood T, Yang PC. Western blot: technique, theory, and trouble shooting. N Am J Med Sci. 2012;4(9):429-34.

87.     Mahmood T, Yang P-C. Western blot: technique, theory, and trouble shooting. North American journal of medical sciences. 2012;4(9):429-34.

88.     ThermoFisher. Chemiluminescent Western Blotting [Available from: https://www.thermofisher.com/no/en/home/life-science/protein-biology/protein-biology-learning-center/protein-biology-resource-library/pierce-protein-methods/chemiluminescent-western-blotting.html.

89.     ThermoFisher. Overview of Western Blotting [Available from: https://www.thermofisher.com/no/en/home/life-science/protein-biology/protein-biology-learning-center/protein-biology-resource-library/pierce-protein-methods/overview-western-blotting.html.

90.     CellTiter-Glo® Luminescent Cell Viability Assay 2015 [Available from: https://www.promega.com/-/media/files/resources/protocols/technical-bulletins/0/celltiter-glo-luminescent-cell-viability-assay-protocol.pdf?la=en.

91.     Rita Hannah MB, Richard Moravec, Terry Riss. CELLTITER-GLO™ LUMINESCENT CELL VIABILITY ASSAY: A SENSITIVE AND RAPID METHOD FOR DETERMINING CELL VIABILITY 2001 [Available from: https://www.promega.com/~/media/Files/Resources/Cell%20Notes/cn002/CellTiter-Glo%20Luminescent%20Cell%20Viability%20Assay-%20A%20Sensitive.ashx.

92.     McKinnon KM. Flow Cytometry: An Overview. Curr Protoc Immunol. 2018;120:5.1.-5.1.11.

93.     Introduction to flow cytometry [Available from: https://www.abcam.com/protocols/introduction-to-flow-cytometry.

94.     Technology [Available from: https://tautechnologies.nl/technology.html.

95.     Annexin V-FITC Apoptosis Detection Kit [Available from: https://www.nacalai.co.jp/global/download/pdf/AnnexinV-FITC.pdf.

96.     eBioscience™ Propidium Iodide [Available from: https://www.thermofisher.com/order/catalog/product/BMS500PI?gclid=Cj0KCQjw4cOEBhDMARIsAA3XDRiaG_yVrkHzKxJk17USfw31Rpm5VrqJDmjPCo-b1BDjt10qjvgxDOwaAiHEEALw_wcB&s_kwcid=AL!3652!3!358436904843!e!!g!!propidium%20iodide&ef_id=Cj0KCQjw4cOEBhDMARIsAA3XDRiaG_yVrkHzKxJk17USfw31Rpm5VrqJDmjPCo-b1BDjt10qjvgxDOwaAiHEEALw_wcB:G:s&s_kwcid=AL!3652!3!358436904843!e!!g!!propidium%20iodide&cid=bid_pca_frg_r01_co_cp1359_pjt0000_bid00000_0se_gaw_nt_pur_con#/BMS500PI?gclid=Cj0KCQjw4cOEBhDMARIsAA3XDRiaG_yVrkHzKxJk17USfw31Rpm5VrqJDmjPCo-b1BDjt10qjvgxDOwaAiHEEALw_wcB&s_kwcid=AL!3652!3!358436904843!e!!g!!propidium%20iodide&ef_id=Cj0KCQjw4cOEBhDMARIsAA3XDRiaG_yVrkHzKxJk17USfw31Rpm5VrqJDmjPCo-

[b1BDjt10qjvgxDOwaAiHEEALw_wcB:G:s&cid=bid_pca_frg_r01_co_cp1359_pjt0000_bid00000_0se_gaw_nt_pur_con](b1BDjt10qjvgxDOwaAiHEEALw_wcB:G:s&cid=bid_pca_frg_r01_co_cp1359_pjt0000_bid00000_0se_gaw_nt_pur_con).

97.     Chesi M, Matthews GM, Garbitt VM, Palmer SE, Shortt J, Lefebure M, et al. Drug response in a genetically engineered mouse model of multiple myeloma is predictive of clinical efficacy. Blood. 2012;120(2):376-85.

98.     Chesi M, Robbiani DF, Sebag M, Chng WJ, Affer M, Tiedemann R, et al. AID-dependent activation of a MYC transgene induces multiple myeloma in a conditional mouse model of post-germinal center malignancies. Cancer Cell. 2008;13(2):167-80.

99.     Meng Q, Ren C, Wang L, Zhao Y, Wang S. Knockdown of ST6Gal-I inhibits the growth and invasion of osteosarcoma MG-63 cells. Biomedicine & Pharmacotherapy. 2015;72:172-8.

100.    Yang Z, Wang S, Halim A, Schulz MA, Frodin M, Rahman SH, et al. Engineered CHO cells for production of diverse, homogeneous glycoproteins. Nature Biotechnology. 2015;33(8):842-4.

101.    Spearman M, Butler M. Glycosylation in Cell Culture. In: Al-Rubeai M, editor. Animal Cell Culture. Cham: Springer International Publishing; 2015. p. 237-58.

102.    Arnold JN, Wormald MR, Sim RB, Rudd PM, Dwek RA. The impact of glycosylation on the biological function and structure of human immunoglobulins. Annual Review of Immunology2007. p. 21-50.

103.    Xue J, Zhu L-P, Wei Q. IgG-Fc N-glycosylation at Asn297 and IgA O-glycosylation in the hinge region in health and disease. Glycoconjugate Journal. 2013;30(8):735-45.
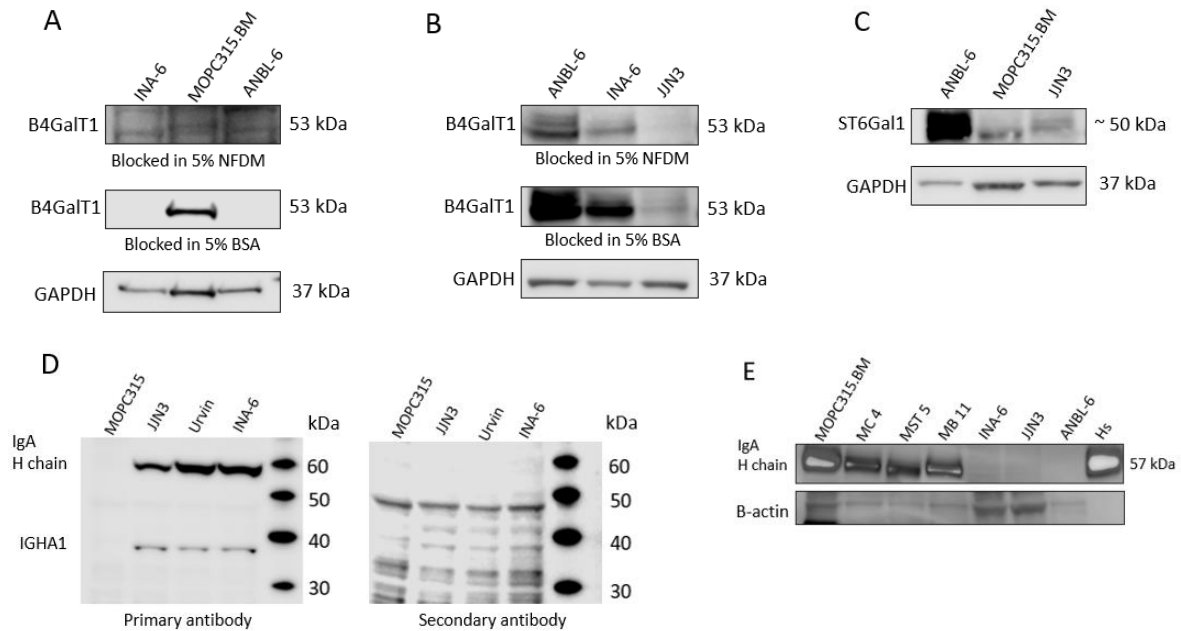
Figure S2. The antibodies used for western blot analysis in this project were tested on cell lysate from human myeloma cell lines (INA-6, ANBL-6, JJN3 and Urvin) and a myeloma mouse cell line, MOPC316.BM, before use. A and B: Two antibodies are required to detect B4GalT1, because the antibody against human B4GalT1 do not detect mice B4GalT1 and vice versa. Testing an anti-mouse B4GalT1 (#DF3839) in A and anti-human B4GalT1 (AF3609) in B. The effect of using, 5% dry milk (NFDM) or 5% BSA as blocking solution were tested. GAPDH is used as loading control. C: Anti ST6Gal1 (AF5924) detects both human and mice ST6Gal1. The blot was blocked in 5% BSA in TBS-T. D: Testing an antibody against the constant region of IgA heavy chain (IGHA1, PA5-86579) on IgA-expressing myeloma cell lines to see if also full-length IgA heavy chain also is detected by this antibody. The primary antibody does indeed bind IgA heavy chain, but it appears to not bind to murine IgA. There seems to be no problematic unspecific binding of the secondary antibody. E: Testing an antibody against IgA heavy chin (ab97235) on cell lysate from MOPC315.BM cells and clones (MC4, MST5, MB11), human cell lines (INA6, JJN3 and ANBL-6) and human serum. The antibody appears to bind to IgA in the mice cell line MOPC315.BM (and clones) and to human serum. Beta-actin is used as loading control.

# Appendix II

Table S1. List of secondary antibodies used in western blot. Antibodies were diluted in 5% BSA in TBS-T.

| Antibody | Manufacturer | Catalog number | Dilution |
|---|---|---|---|
| Polyclonal Goat Anti-Rabbit Immunoglobulins/HRP | Agilent Dako | P0448 | 1:3000 |
| Polyclonal Rabbit Anti- Goat Immunoglobulin/HRP | Agilent Dako | P0449 | 1:2000 |
| Polyclonal Goat Anti-Mouse immunoglobulin/HRP | Agilent Dako | P0447 | 1:3000 |
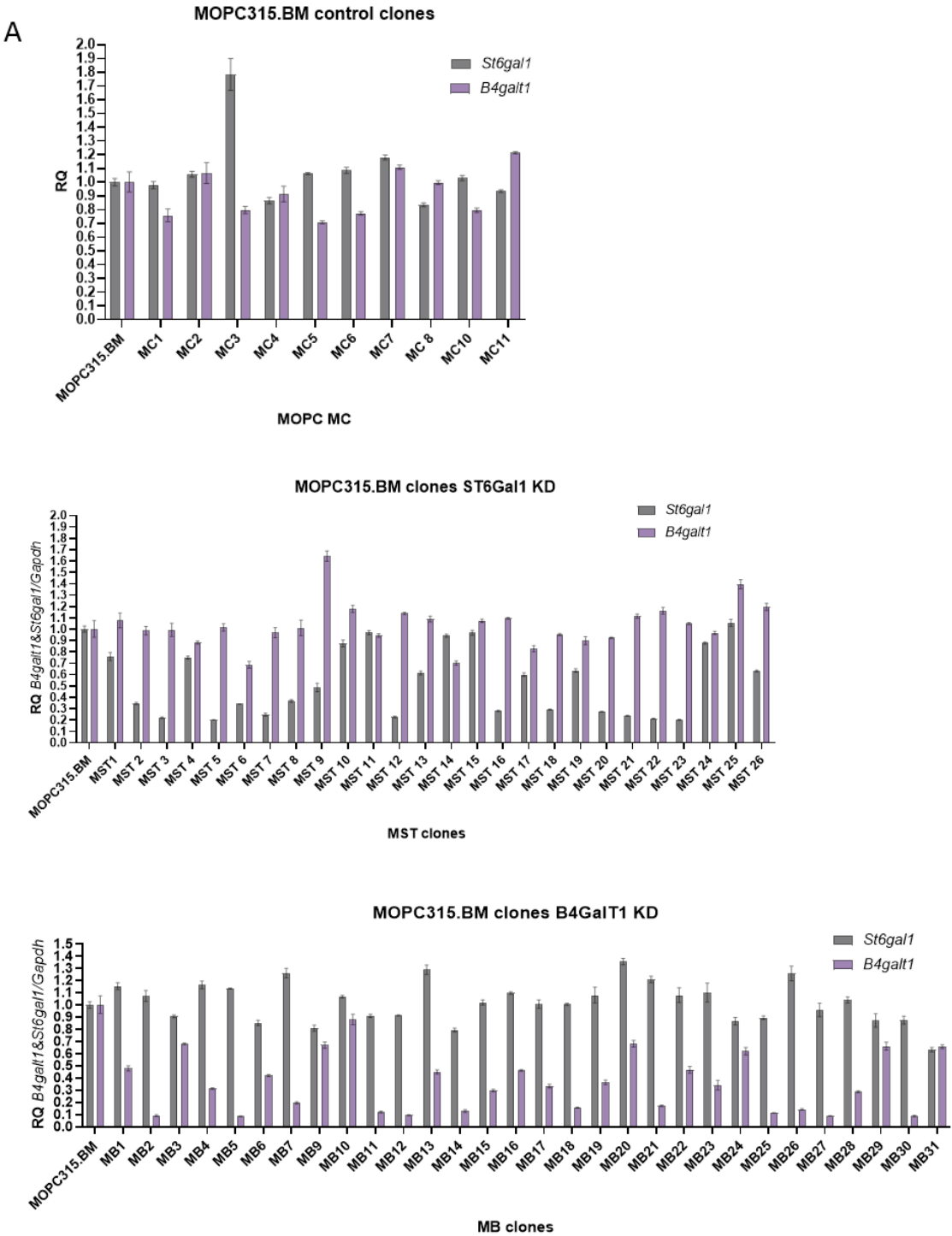
Figure S3. The gene expression of St6gal1 and B4galt1 in MOPC315.BM, STGal1/B4GalT1 KD clones and control clones was analyzed by qPCR. MOPC315.BM was used as "reference sample" and GAPDH is the endogenous control. The control clones, ST6Gal1 KD clones and B4GalT1 KD are plotted in graph A, B and C, respectively.

# Appendix IIII
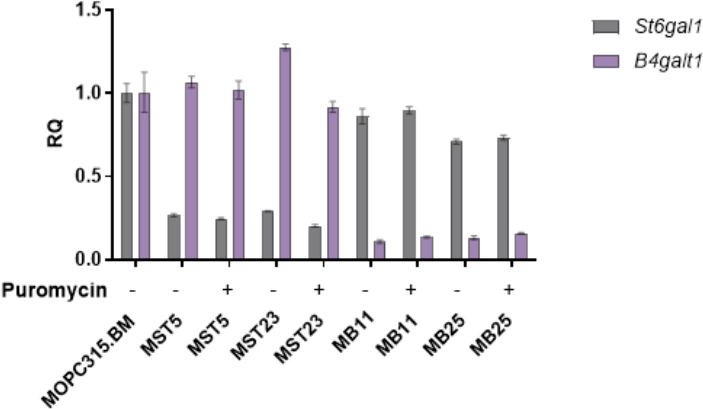


Figure S4. qPCR of the selected clones after they were grown with and without puromycin for ten days. MOPC315.BM is used as "reference sample" and beta-actin is the endogenous control. The control clones are not represented in the graph, due to poor RNA quality caused by a closing of the lab because of the Corona situation.